Accepted Manuscript

Pancreatic ductal deletion of *Hnf1b* disrupts exocrine homeostasis, leads to pancreatitis and facilitates tumorigenesis

Evans Quilichini, Mélanie Fabre, Thassadite Dirami, Aline Stedman, Matias De Vas, Ozge Ozguc, Raymond C. Pasek, Silvia Cereghini, Lucie Morillon, Carmen Guerra, Anne Couvelard, Maureen Gannon, Cécile Haumaitre

PII: S2352-345X(19)30084-0
DOI: https://doi.org/10.1016/j.jcmgh.2019.06.005
Reference: JCMGH 496

To appear in: *Cellular and Molecular Gastroenterology and Hepatology*
Accepted Date: 13 June 2019

Please cite this article as: Quilichini E, Fabre M, Dirami T, Stedman A, De Vas M, Ozguc O, Pasek RC, Cereghini S, Morillon L, Guerra C, Couvelard A, Gannon M, Haumaitre C, Pancreatic ductal deletion of *Hnf1b* disrupts exocrine homeostasis, leads to pancreatitis and facilitates tumorigenesis, *Cellular and Molecular Gastroenterology and Hepatology* (2019), doi: https://doi.org/10.1016/j.jcmgh.2019.06.005.

This is a PDF file of an unedited manuscript that has been accepted for publication. As a service to our customers we are providing this early version of the manuscript. The manuscript will undergo copyediting, typesetting, and review of the resulting proof before it is published in its final form. Please note that during the production process errors may be discovered which could affect the content, and all legal disclaimers that apply to the journal pertain.

ACCEPTED MANUSCRIPT

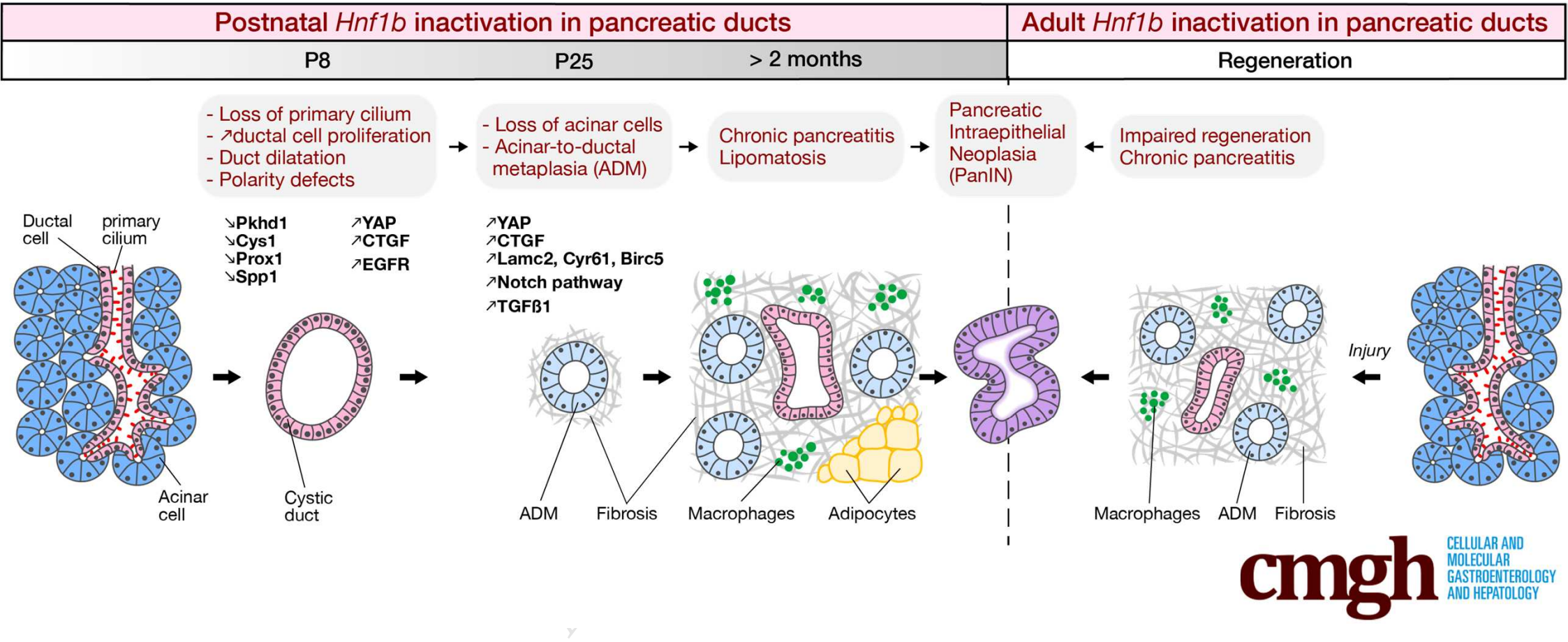

cmgh CELLULAR AND MOLECULAR GASTROENTEROLOGY AND HEPATOLOGY

ACCEPTED MANUSCRIPT

Pancreatic ductal deletion of *Hnf1b* disrupts exocrine homeostasis, leads to pancreatitis and facilitates tumorigenesis

Short title. ***Pancreatitis due to ductal Hnf1b inactivation***

Evans Quilichini[1], Mélanie Fabre[1], Thassadite Dirami[1#], Aline Stedman[1#], Matias De Vas[1], Ozge Ozguc[1], Raymond C. Pasek[2], Silvia Cereghini[1], Lucie Morillon[1], Carmen Guerra[3], Anne Couvelard[4], Maureen Gannon[2], Cécile Haumaitre[1*]

Affiliations

[1] Sorbonne Université, Centre National de la Recherche Scientifique (CNRS), Institut de Biologie Paris-Seine (IBPS), F-75005 Paris, France

[2] Department of Medicine, Vanderbilt University Medical Center, Nashville, Tennessee, USA

[3] Molecular Oncology Program, Centro Nacional de Investigaciones Oncológicas (CNIO), Madrid 28029, Spain.

[4] Hôpital Bichat, Département de Pathologie, Assistance Publique-Hôpitaux de Paris, Université Paris Diderot, F-75018 Paris, France

# Equal contribution

* Corresponding author.

ACCEPTED MANUSCRIPT

Grant support

Support to CH was received from the Centre National de la Recherche Scientifique (CNRS), the Universite Pierre et Marie Curie (UPMC)- Sorbonne Université , the GEFLUC - Les entreprises contre le Cancer, the Societe Francophone du Diabete (SFD)-Ypsomed, the programme Emergence UPMC. EQ was supported by a PhD fellowship from the French Ministère de la Recherche et de la Technologie. MF is an assistant engineer of the CNRS. TD and AS were supported by Sorbonne Université. MDV was supported by a PhD student fellowship from the European Marie Curie Initial Training Network (ITN)-Biology of Liver and Pancreatic Development and Disease (BOLD). O. O. was supported by a Master1 fellowship. RCP was supported by a postdoctoral fellowship from the American Heart Association (14POST20380262). MG was supported by the National Institutes of Health (U01 DK089540) and the Juvenile Diabetes Research Foundation (1-2011-592). CH is a permanent senior researcher of the Institut National de la Sante et de la Recherche Medicale (INSERM).

Abbrevations

ADM, acinar-to-ductal metaplasia; AcTub, acetylated α-tubulin; ECM, extracellular matrix; EMT, epithelial-mesenchymal transition; H&E, hematoxylin & eosin; PanIN, pancreatic intraepithelial neoplasia; PDAC, pancreatic ductal adenocarcinoma; PPH3, phospho-histone H3; PSC, pancreatic stellate cell; α-SMA, α-smooth muscle actin; TM, tamoxifen; TUNEL, terminal deoxynucleotidyltransferase-mediated dUTP-biotin nick end labeling.

Correspondence :

Cecile Haumaitre

Sorbonne Université, Centre National de la Recherche Scientifique (CNRS), Institut de Biologie Paris-Seine (IBPS), 9 Quai Saint-Bernard, Batiment C - 7eme etage - case 24. 75252 PARIS Cedex 05, FRANCE.

Phone : +33 1 44 27 21 51, Fax : +33 1 44 27 34 45. Email : cecile.haumaitre@inserm.fr

Author contributions :

EQ, MF, TD, AS, MDV, OO, RP, LM, CH performed experiments; EQ, TD, AS, MDV, OO, LM, AC, CH analyzed and interpreted data; SC, CG, MG provided materials; CH wrote the manuscript; EQ, AS, MDV, RP, SC, CG, AC, MG revised the manuscript; CH designed and supervised the study, obtained funding.

Word count: (not included abstract, methods, figure legends and references): 5916

Synopsis

This study shows how *Hnf1b* inactivation in pancreatic ductal cells leads to chronic pancreatitis, neoplasia and potentiates PanIN formation. This reveals a cause of pancreatitis and identifies Hnf1b as potential tumor suppressor for pancreatic cancer.

Abstract

Background and aims. The exocrine pancreas consists of acinar cells that produce digestive enzymes transported to the intestine through a branched ductal epithelium. Chronic pancreatitis is characterized by progressive inflammation, fibrosis and loss of acinar tissue. These changes of the exocrine tissue are risk factors for pancreatic cancer. The cause of chronic pancreatitis cannot be identified in one-quarter of patients. Here, we investigated how duct dysfunction could contribute to pancreatitis development.

Methods. The transcription factor Hnf1b, first expressed in pancreatic progenitors, is strictly restricted to ductal cells from late embryogenesis. We have previously shown that Hnf1b is crucial for pancreas morphogenesis but its postnatal role still remains unelucidated. To investigate the role of pancreatic ducts in exocrine homeostasis, we inactivated *Hnf1b* gene *in vivo* in mouse ductal cells.

Results. We uncovered that postnatal *Hnf1b* inactivation in pancreatic ducts leads to chronic pancreatitis in adults. *Hnf1b*Δ^{duct} mutants display dilatation of ducts, loss of acinar cells, acinar-to-ductal metaplasia (ADM) and lipomatosis. We deciphered the early events involved, with downregulation of cystic disease-associated genes, loss of primary cilia, upregulation of signaling pathways, especially Yap pathway involved in ADM. Remarkably, *Hnf1b*Δ^{duct} mutants developed pancreatic intraepithelial neoplasia and promote PanIN progression in concert with KRAS. We further showed that adult *Hnf1b* inactivation in pancreatic ducts is associated with impaired regeneration after injury, with persistent metaplasia and initiation of neoplasia.

Conclusion. Loss of *Hnf1b* in ductal cells leads to chronic pancreatitis and neoplasia. This reveals that *Hnf1b* deficiency may contribute to diseases of the exocrine

pancreas and could gain further insight into the etiology of pancreatitis and tumorigenesis.

Keywords

Pancreatitis, Pancreatic cancer, Hnf1b, Ducts, Acinar-to-ductal-metaplasia

ACCEPTED MANUSCRIPT

Introduction

Pancreatitis is a common disorder with significant morbidity and mortality, yet little is known about its pathogenesis, and there is no specific or effective treatment. It is characterized by progressive inflammation, necrosis/apoptosis, fibrosis, loss of acinar tissue and acinar-to-ductal metaplasia (ADM). Chronic pancreatitis increases the risk of pancreatic cancer [1]. Pancreatic ductal adenocarcinoma (PDAC) is one of the most lethal malignancies in humans, occurring through the progression of precursor lesions, the best described being pancreatic intraepithelial neoplasia (PanIN). ADM is critical in neoplastic transformation, since metaplastic acinar cells can undergo the reprogramming process from ADM to form PanINs [2,3]. Fibrosis also provides the background for PanIN development [4].

The major etiologies of pancreatitis are obstruction of the pancreatic duct usually due to gallstones, alcohol, and smoking. Pancreatitis has also been associated with genetic factors, including mutations of cystic fibrosis transmembrane regulator *(*CFTR*)* gene, as well as PRSS1, SPINK-1, CTRC, CLDN2. However, the cause of chronic pancreatitis cannot be identified in about 30% of patients [4].

The exocrine compartment of the pancreas consists of acinar cells that secrete enzymes and an intricate system of epithelial ductal cells that secrete the fluid carrying the digestive enzymes in the gut. Ductal cells comprise centroacinar cells, intercalated intralobular and interlobular ducts, linking the acinar lobules to the main pancreatic duct that drains into the duodenum [5]. In vertebrates, pancreatic duct morphogenesis initiates with the formation of a network of primitive ducts, which matures into a tubular system. A restricted set of transcription factors are involved in ductal cell differentiation such as Sox9 and Hnf1b [5,6]. Whereas acinar cells are not ciliated, ductal

cells harbor an immotile primary cilium [7–9]. These microtubule-based organelles projecting from the surface of the pancreatic ductal cells function as chemo- and mechano-sensors and integrate multiple signaling pathways [10]. Except for duct obstruction and mutations in CFTR gene, duct contribution in acinar cell homeostasis is poorly known and the cellular and molecular mechanisms leading to acinar damage and chronic pancreatitis are poorly understood.

In the present study, we investigate how duct dysfunction may contribute to pancreatitis. We focused on the transcription factor Hnf1b, which presents a very interesting profile. It is first expressed in pancreatic progenitors, then restricted to ductal cells from late embryogenesis such as only few transcription factors, and so not expressed in acinar cells [11–13]. We have previously shown that Hnf1b is crucial for duct morphogenesis during embryogenesis [13]. Here, we investigate its role in differentiated ducts after birth. In the post-natal pancreas, acinar cells do not derive from ducts [12,14,15], allowing analysis of the role of Hnf1b in duct function and the consequences on acinar cell homeostasis.

Our data show that Hnf1b has a crucial function in the regulatory network controlling differentiated epithelial ductal cells and maintenance of the primary cilium. Its ductal function is critical to maintain acinar homeostasis as loss of Hnf1b in ductal cells leads to chronic pancreatitis and neoplasia. Thus, *Hnf1b* deficiency causes dysfunction of the exocrine pancreas, providing further insights into the etiology of pancreatitis and a risk factor for tumorigenesis.

ACCEPTED MANUSCRIPT

Results

Post-natal inactivation of Hnf1b in pancreatic ducts leads to loss of primary cilia and cystic duct formation

To perform a postnatal conditional inactivation of *Hnf1b* in ductal cells, we generated Sox9-CreER;Hnf1b$^{fl/fl}$;R26R^{YFP} mutants and conditionally inactivated *Hnf1b* during the first three days after birth (P1-P3), further mentioned as *Hnf1b*Δ^{duct} mutants. We analyzed the consequences on pancreata dissected 5 days after the last tamoxifen injection, at P8. We assessed that *Hnf1b* inactivation in pancreatic ductal cells was efficient by RT-qPCR, showing a 65% decrease in *Hnf1b* expression in mutants (Figure 1A). By immunostaining, we observed nuclear Hnf1b localization in ductal structures in controls (Figure 1B-C), whereas Hnf1b was absent from GFP positive ducts in mutants. Hnf1b protein persisted in only 14% of non-recombined ducts, negative for GFP (Figure 1D).

As a transcription factor, Hnf1b controls a network of genes involved in duct morphogenesis during development [13]. In order to investigate the role of *Hnf1b* in differentiated ducts after birth, we analyzed the expression of genes involved in the maintenance of the primary cilium and in ductal cell integrity and functionality (Figure 1E). In *Hnf1b*Δ^{duct} mutants, we found by RT-qPCR a significant decrease in expression of cystic disease genes, known as direct targets of Hnf1b in renal cells or in pancreatic progenitors [13-17]. We observed a strong decrease in *Pkhd1*, *Cys1, Spp1 and Prox1* expression, involved in ciliary maintenance and/or tubular architecture [18-21]. *Tg737/Ift88* required for ciliogenesis was also significantly downregulated. By contrast, the expression of the ductal markers *Sox9*, *Hnf6* and *Ck19* was unchanged compared to

controls, showing that ductal cell differentiation is maintained. Moreover, expression of *Cftr* was unaffected in *Hnf1b*Δ^{duct} mutants.

As we found a specific downregulation of genes involved in the maintenance of the ductal primary cilium, we examined primary cilia in *Hnf1b*Δ^{duct} mutants. Immunostaining of acetylated α-tubulin (AcTub), a tubulin modification present on primary cilium axonemes, revealed a loss of cilia in ductal cells of *Hnf1b*Δ^{duct} mutants (Figure 1F, G). This was confirmed by the absence of Arl13b immunostaining, a cilium-specific membrane protein (Figure 1H, I). Quantification showed a 73% decrease in ciliated ductal cells in *Hnf1b*Δ^{duct} mutants (Figure 1J), in agreement with the level of *Hnf1b* inactivation efficiency. To correlate *Hnf1b* inactivation and the loss of the primary cilium at the cellular level, we performed AcTub/GFP co-immunostainings. *Hnf1b*-inactivated ducts labeled with GFP do not present any cilia (Figure 1K-M).

As loss of cilia may promote aberrant cell division, permitting increased proliferation [22], we quantified proliferation of ductal cells by Sox9/Phospho-histone H3 (PPH3) immunostainings (Figure 1N-O). Mutant ducts presented more proliferative cells than control pancreatic ducts (1.4-fold) (Figure 1P). This resulted in a significant increase of the ductal cell area (1.2-fold) quantified by the number of Sox9+ cells (Figure 1Q).

We investigated if these abnormalities could lead to cyst formation. By Hematoxylin & Eosin (H&E) staining, we observed dilated ducts in *Hnf1b*Δ^{duct} mutants (Figure 1R, S). Sox9 and Hnf6 exhibited nuclear staining of enlarged mutant ductal structures (Figure 1T, U and data not shown), showing that dilated ducts still express some terminal differentiation markers. We further analyzed ductal cell polarity. Control ducts showed strong apical localization of Muc1 and PKCz in epithelial cells around the duct lumen (Figure 1V-Y). In *Hnf1b*Δ^{duct} mutants, this apical staining persisted in non-

dilated ducts (Figure 1W') whereas it was reduced and discontinuous in the cells lining cysts in mutants (Figure 1W''). Whereas the Spp1/osteopontin matricellular protein was localized on the apical side of control ductal cells, we observed very few Spp1+ cells in mutants, confirming RT-qPCR results (Figure 1Z, AA).

Altogether, these results show that Hnf1b has a prominent role in the regulatory network controlling the maintenance of the primary cilium and tubular architecture of pancreatic ducts after birth.

Post-natal inactivation of Hnf1b in pancreatic ducts leads to non-cell autonomous effects on acinar cells through activation of the YAP mechano-transducer

A direct antagonistic interaction between ciliogenesis and YAP function has been shown [23]. YAP activation was also observed in hepatic cystogenesis associated with *Pkhd1* deficiency [24]. YAP has a central role as mechano-effector and sensor of cell polarity, being a mediator of mechanical cues and linking the physicality of cells and tissues to potent transcriptional responses. It is mechanically regulated by various regimens of cell stretching, such as deformations of epithelial monolayers [25-27]. In *Hnf1b*Δ^{duct} mutants, we visualized the deformation of pericystic areas with an immunostaining of the fibroblast marker α-smooth muscle actin (α-SMA) at P8. While α-SMA+ cells were restricted around blood vessels in control pancreata (Figure 2A), mutants exhibited widespread α-SMA staining showing activation of fibroblasts surrounding ducts and in periacinar spaces (Figure 2A, B). Interestingly, we observed an increased number of cells with YAP nuclear staining in *Hnf1b*Δ^{duct} mutants in pericystic and acinar areas (Figure 2C-F). Consistent with YAP activation, we found a strong increase in YAP transcriptional targets, with upregulation of *Ctgf* (1.8-fold) and *Lamc2* in

*Hnf1b*Δ^{duct} mutants compared to controls (Figure 2G). To determine in which cell type we observed the YAP nuclear enrichment, we performed co-immunostainings for YAP/Sox9 and YAP/Amylase to analyze ductal and acinar cells respectively. While in controls YAP localized only in the nucleus of Sox9+ ductal cells (Figure 2H-M), in mutants, it localized also ectopically in Amylase+ acinar cells (Figure 2N-S), suggesting that mechanical stress induced by enlarging cysts stimulates YAP activation in acinar cells at P8. These data show cell autonomous and non-cell autonomous upregulation of the YAP pathway when *Hnf1b* is inactivated in ductal cells.

Post-natal inactivation of Hnf1b in ducts leads to acinar-to-ductal metaplasia, loss of acinar cells and lipomatosis

YAP nuclear localization and increased expression of the YAP target gene Ctgf is particularly interesting because of its involvement in ECM fibrosis [28,29]. Accordingly, we observed a marked increase in periductal collagen deposition as indicated by histological analysis with Masson's Trichrome at P8 (Figure 3A, B; green areas). These changes are reminiscent of pancreas fibrosis, which is often associated with ADM. As it was recently shown that YAP activity is necessary and sufficient for ADM and pancreatitis induction [30-32], we examined whether acinar cells were secondarily affected in mutants. Whereas we found no significant changes in acinar gene expression by RT-qPCR at P8 (Figure 3C), we already observed at this stage a 41% decrease in the number of Amylase+ cells (Figure 3D). We found an upregulation of *EGFR* expression in mutants (1.6-fold), whereas *TGFβ-1* remained unchanged at this stage (Figure 3E), both known to promote ADM [33-35]. Moreover, Amylase/PPH3 immunostaining quantifications revealed a 47% decrease in acinar cell proliferation (Figure 3F-H), whereas TUNEL assay showed

a 15.5-fold increase in acinar cell apoptosis (Figure 3I-K) in mutants compared to controls. Hence, a combined reduction in acinar cell proliferation and an increase in apoptosis leads to acinar cell loss. Then, large areas of ADM were observed at P25 in mutants (Figure 4A, B), associated with a dramatic decrease in acinar gene expression (89% for amylase, Figure 4I) and a strong upregulation of Sox9 (2.2-fold, Figure 4J). Moreover, Sox9 and Hnf6 were ectopically expressed in some acinar cells in mutants (Figure 4E-H), characterizing ADM [36]. As previously shown in a model of TGF-β induced ADM [37], we also found an ectopically induced Hnf1b expression in acinar cells at P25 (Figure 4C, D). At this stage, ducts were more affected than at P8 as indicated by the complete loss of Muc1 apical staining in mutants (Figure 4K-L), which corroborated with the dramatic decrease in *Muc1* transcript levels (Figure 4J). We found a 55% decrease in *Hnf6* expression (Figure 4J), with few Hnf6+ cells remaining in mutants ducts compared with ductal Sox9+ cells (Figure 4C-F), in agreement with our finding that *Hnf6* is a direct target of Hnf1b during pancreas development [13]. By Amylase/Pan-CK co-immunostainings, acinar structures appear closely connected with this ductal network and more importantly Pan-CK co-localized with some Amylase+ cells in mutants (Figure 4M, N). We noticed sparse area with fat infiltration only in mutants and identified that these fat-containing cells were adipocytes using the Fabp4 marker (Figure 4O-P), fatty replacement of pancreatic parenchyma being often associated with pancreatic fibrosis and pancreatitis [4]. YAP pathway was dramatically upregulated in mutants, stronger than at P8: 8.6-fold for *Ctgf,* 6.3-fold for *Lamc2* and 2.8-fold for *Cyr61* (Figure 4Q). The Notch pathway was shown to be activated during acinar dedifferentiation and to promote ADM [38]. We found an upregulation of most of Notch components (Figure 4R), and especially a 2.4-fold increase in *Notch2* expression, a receptor confined to ducts by E15.5 [39]. Moreover, we observed a significant increase in

Jag1 expression, which was shown to be upregulated in expanded ducts of chronic pancreatitis patients [40]. At this stage, we also observed a strong increase (3.6-fold) in *TGF-β1* expression in mutants and a significant increase in *p8/Nupr1* expression (Figure 4S), a transcriptional cofactor expressed at only low levels in normal pancreata but induced in the initial phases of pancreatitis [41].

Hence, *Hnf1b* loss of function in ducts leads to loss of acinar cells and ADM, as well as lipomatosis in the pancreas, together with the upregulation of Yap, Notch and TGF-β1 pathways.

Post-natal inactivation of Hnf1b in ducts leads to chronic pancreatitis in adults

We further investigated the progression in adults of the pancreatic exocrine disorder associated with ductal *Hnf1b*-deficiency. We observed a 43% decrease in pancreas weight at 2 months in mutants, whereas mouse weight was unchanged compared to controls (Figure 5A). At 5 months, mouse weight was significantly decreased in mutants as a consequence of pancreatic exocrine deficiency (data not shown). The decreased pancreatic weight was correlated with a dramatic loss of acinar tissue (Figure 5B, C) correlated with a 95% decrease in acinar gene expression (Figure 5I). Many lobes of *Hnf1b*Δ^{duct} mutant pancreata were entirely devoid of acinar tissue and merely consisted of isolated ducts embedded within a large mass of fat. Extensive ADM was demonstrated by very few acini scattered in the tissue and displaying enlarged lumen (Figure 5E), duct-like structures (Figure 6F) and a strong Sox9 ectopic localization in acinar cells (Figure 5G-H). Mutant pancreata displayed inflammation (Figure 5J). We observed a dramatic increase in *F4/80* expression, a marker of macrophages, and in CD2 expression, a marker of T cells, whereas expression of CD19, a

marker of B cells was unchanged (Figure 5K). In correlation, we found an upregulation of CCL2, CCL5 and CXCL10, showing the involvement of these chemokines in the mutant inflamed pancreas. Infiltration of macrophages was also observed by F4/80 immunostaining (Figure 5L, M), having important role in the pathogenesis of pancreatitis. Moreover, extensive lipomatosis was observed in mutants (Figure 5J). Fabp4 immunostaining showed extended areas of adipocytes (Figure 5N, O) and *PPARg* expression, a key player in adipocyte differentiation [42], was dramatically increased (16.6-fold) in mutants (Figure 6P). The pancreatic parenchyma of the mutant was replaced by fibrotic tissue as shown by Masson's Trichrome (Figure 5Q, R) and a 10.2-fold increase in the expression of the desmoplasia-associated marker *Col1A1* in mutants (Figure 5S). We observed a 12.8-fold increase in *α-SMA* expression in mutants, showing pancreatic stellate cell (PSC) activation, a key mediator in the fibrosis observed in the desmoplastic reaction [43] (Figure 5V). Interestingly, we found a strong accumulation of the mesenchymal-related protein Vimentin in mutants (Figure 5T, U) correlated with a dramatic increase in *Vimentin* expression (47.7-fold) (Figure 5V), as well as up-regulation of another mesenchymal marker N-cadherin (5.5-fold). Inversely, the epithelial marker E-cadherin was dramatically downregulated (87%), showing epithelial-mesenchymal transition (EMT).

Thus, inflammation, fibrosis, activation of PSCs and EMT promote chronic pancreatitis in adult *Hnf1b*Δ^{duct} mutants.

Post-natal inactivation of Hnf1b in ducts leads to pancreatic neoplasia and potentiates Kras^{G12V} -driven PanIN formation

Chronic pancreatitis has been shown to predispose to pancreatic cancer [1]. Activated signaling pathways play a role in ADM and also in early PanIN lesions. We therefore investigated potential development of PanINs in adult *Hnf1b*Δ^{duct} mutants.

CTGF production is abundant in the desmoplastic stroma present in pancreatic cancer [44]. We found a 4.4-fold increase of *Ctgf* expression in adult *Hnf1b*Δ^{duct} mutants (Figure 6A), and strong ectopic CTGF protein localization in acinar cells in mutants compared to controls (Figure 6B, C). Moreover, we observed strong CTGF expression in the epithelium of metaplastic ducts (Figure 6D) and in neoplastic lesions (Figure 6E) in *Hnf1b*Δ^{duct} mutants. *Cyr61* was recently reported to be expressed in PanINs, Cyr61 signaling being critical for EMT and promoting pancreatic carcinogenesis [45]. We found a dramatic increase (6.1-fold) of *Cyr61* in adult *Hnf1b*Δ^{duct} mutants, as well as *Lamc2* and *Birc5*, other markers of the YAP pathway (Figure 6A).

TGF–β pathway activation plays a crucial role in pancreatic tumor initiation through its capacity to induce ADM, providing a favorable environment for neoplasia [37]. We found a 12.8-fold increase in *TGF-β1* expression in mutants compared to controls (Figure 6F), with a 4-fold increase compared to mutants at P25. Moreover, Phospho-Smad2 protein was strongly ectopically localized in the nuclei of ADM structures, metaplastic ducts and fibrotic tissue (Figure 6G, H), monitoring the activation of the TGF-β signaling pathway in adult *Hnf1b*Δ^{duct} mutants.

Ectopic Notch activation, promoting both initiation and progression of PanINs, is also an early event in pancreatic carcinogenesis [46]. We found a strong up-regulation of Notch pathway components, higher than at P25 especially for the receptor *Notch2* and the effector *Hey2*, (6.4-fold and 5.9-fold respectively, Figure 6I). In correlation, Hey2 protein was observed ectopically in acinar cells, in enlarged ducts and in ADM structures in mutants (Figure 6J, K). Aberrant activation of EGFR signaling is also essential in

pancreatic tumorigenesis [34] and we observed a strong up-regulation of *EGFR* (2.3-fold; Figure 6L) in adult *Hnf1b*Δ^{duct} mutants, along with a strong localization of Phospho-AKT in the fibrotic and inflamed tissue of the mutant pancreas (Figure 6M, N).

Remarkably, histological analysis showed intraepithelial neoplasia as low-grade PanINs in *Hnf1b*Δ^{duct} mutant pancreata (Figure 7A). These were characterized by an epithelium composed of tall columnar cells with basally located nuclei with light atypia, a pseudostratified architecture and abundant supranuclear mucin. These neoplastic structures were Alcian Blue-positive (Figure 7B) and positive for the PanIN-specific marker Claudin18 (Figure 7C). Thus, loss of *Hnf1b* leads to pancreatic neoplasia by 2 months. By GFP immunostainings, we performed a lineage tracing analysis and found no GFP signal in ADM/PanIN in Hnf1b mutants strongly suggesting that PanIN like structures derived indirectly from Hnf1b-ablated YFP+ ductal cells, by a non-cell autonomous mechanism (Figure 7 D).

By quantification of the acinar compartment in mutants, 11.6% of remaining acini, 80.8% of adipocytes, 6.1% of fibrosis/infiltrates, 1.3% of ADM and 0.5% of PanIN were observed in mutants (Figure 7E). By analyzing older animals until 18 months, we did not observe PanIN progression (data not shown). We then investigated if loss of Hnf1b could promote tumorigenesis in a context of oncogenic Kras (Kras^{G12V}). Somatic activating mutations in Kras indeed appear in 97% of PDAC patients, but additional factors are required to initiate PanIN progression and PDAC. To activate Kras in acinar cells, we used the Elas-tTA; TetO-Flpase; FRT-Stop-FRT Kras^{G12V} mouse line. Untreated mice (without doxycycline) develop PanIN lesions with long latency, with low grade PanIN from 5/6 months. We crossed these mice, hereafter referred to as Kras, with Sox9-CreER;Hnf1b$^{fl/fl}$ Mutants to obtain Elas-tTA; TetO-Flpase; FRT-Stop-FRT Kras^{G12V}/ Sox9-CreER;Hnf1b $^{fl/fl}$ with TM induction perinataly, hereafter referred to as Kras;

Mutants. Histological analyses by HE staining (Figure 8A), Alcian Blue staining (Figure 8B), and Claudin 18 immunohistochemistry (Figure 8C) at 5 months showed large area of PanINs in Kras;Mutants compared to mutants and age-matched Kras, affecting more lobules with very large amount of lesions. This showed that combination of Hnf1b deletion with oncogenic KRAS activation enhanced pancreatic damage at 5 months relative to oncogenic KRAS alone. Quantification of Alcian Blue positive lesions showed a dramatic increase in the surface of lesions in Mutant;Kras compared to mutants and Kras (Figure 8D), which was due to a combined increase in the number of lesions (Figure 8E) and in the size of the lesions (Figure 8F) in Mutant;Kras. Moreover, we observed an increased progression of PanIN lesions up to high grade at 5 months in Mutant;Kras (Figure 8G-K). Thus, Hnf1b inactivation in ducts provides a propitious environment for the onset of $KRAS^{G12D}$-induced PanINs.

Adult inactivation of Hnf1b in ducts leads to impaired acinar regeneration following caerulein-induced pancreatitis

We next tested the hypothesis that *Hnf1b* could be required for maintenance of exocrine homeostasis in the adult. We inactivated *Hnf1b* in adult ductal cells, with TM injections on 6-weeks old mice and observed the consequences on the pancreatic tissue at 9 weeks and 20 weeks. We did not observed changes in pancreatic weight in these mutants compared to controls (Figure 9A,C). Analysis of acinar marker expression by RT-qPCR (Figure 9B, D) and H&E stainings (Figure 9E,F) yielded no overt pancreatic pathology at either time point when *Hnf1b* was inactivated in adult ducts, probably due to the lower proliferation rate of adult ductal cells compared to post-natal ductal cells [5]. Thus, we investigated if loss of *Hnf1b* in adults would sensitize acinar cells to injury-induced reprogramming, as ductal cells are capable of contributing to acinar

regeneration [47,48]. Two weeks post-TM in adults, acute pancreatitis was induced by 2 consecutive days of treatment with the secretagogue cerulein, and pancreata were harvested 1 week later (D7). We verified that *Hnf1b* inactivation was also efficient at this stage, and observed a 50% decrease in *Hnf1b* expression in *Hnf1b*Δ$^{\text{adult duct}}$ mutants (Figure 10A). We followed *Amylase* expression by RTq-PCR and found no significant changes between controls and mutants at D0 and D3. *Amylase* expression was dramatically decreased at D3, showing the efficiency of the cerulein treatment (Figure 10B). Whereas controls showed a recovery of *Amylase* expression at D7, *Hnf1b*Δ$^{\text{adult duct}}$ mutants were unable to recover after injury, showing dramatically low levels of *Amylase* expression in mutants (99% decrease). Other acinar markers displayed the same pattern of expression with critically low levels of *CPA*, *Ptf1a*, *Mist1* and *Nr5a2* expression in *Hnf1b*Δ$^{\text{adult duct}}$ mutants compared to controls at D7 (Figure 10C). In mutants, we observed a dramatic increase in *F4/80* and CD2 expression, whereas expression of the B cell marker CD19 was unchanged (Figure 10D), showing a increased severity of pancreatitis in mutants with macrophages and T cells recruitment. We found a tendency but not a significant increase in the mRNA level of CCL2, CCL5 and CXCL10 chemokines in mutants at D7, suggesting that the chronic pancreatitis was more established in Hnf1b mutant at 5 months after perinatal inactivation (Figure 5K), than in adult Hnf1b mutants 7 days after cerulein treatment (Figure 10D). Histological analysis by H&E and Masson's Trichrome showed no abnormalities at D0, but ADM and interstitial fibrosis at D3 both in controls and mutants. At D7, whereas control pancreata were recovered, we observed persistent and strong defects in *Hnf1b*Δ$^{\text{adult duct}}$ mutant pancreata, characteristic of chronic pancreatitis (Figure 10E). No large Amylase+ acinar clusters were detected in *Hnf1b*Δ$^{\text{adult duct}}$ mutant pancreata in contrast to controls, and co-localisation of Sox9 and Amylase was observed in almost all acinar cells in *Hnf1b*Δ$^{\text{adult duct}}$ mutant pancreata

(Figure 10F, G), showing widespread ADM at D7. Remarkably, we observed abundant persistent metaplastic lesions, fibrosis, and formation of neoplastic lesions, as shown by histology on H&E (Figure 10H, I), alcian-blue stainings (Figure 10J, K), and by immunohistochemistry with the PanIN-specific marker Claudin18 (Figure 10L, M). These results show the requirement of Hnf1b in adult ducts for acinar cell regeneration in the context of tissue injury. Our data further suggest that *Hnf1b* deficiency in adult ductal cells in the context of tissue injury can initiate neoplastic lesions.

Discussion

We show that *Hnf1b* inactivation in ductal cells after birth causes loss of primary cilia, duct proliferation and dilatation. This triggers fibrosis, ADM, inflammatory infiltration, lipomatosis, activation of PSC and EMT, leading to chronic pancreatitis and PanINs.

Hnf1b-inactivation in differentiated post-natal pancreatic ducts leads to chronic pancreatitis

Ductal *Hnf1b* inactivation leads to dramatic decrease in cystic-disease associated gene expression, especially *Pkhd1* and *Cys1*, reinforcing our previous findings that they were direct targets of Hnf1b in pancreatic progenitors at E12.5 [13]. *Pkhd1*, *Cys1*, and *Tg737/Ift88* play a role in the structural integrity of cilia. The *Pkhd1* gene encodes Fibrocystin, a membrane protein localised to the primary cilium of tubular epithelial cells [49] and lack of Fibrocystin disrupted ciliogenesis in *Pkhd1*-deficient mice [50]. Interestingly, it was recently reported novel mutations of *PKHD1* associated with

chronic pancreatitis [51]. The *Cys1* gene product, Cystin, also localizes to the primary cilium and stabilizes microtubule assembly [52]. The protein IFT88/polaris is a core component of the intraflagellar transport machinery and is required for the formation of cilia [53]. Primary cilia transduce signals from extracellular stimuli to a cellular response that regulates proliferation, differentiation, transcription, migration, polarity and tissue morphology [54]. They can play a negative role in epithelial cell proliferation [55]. Mutations affecting cilia development promote a dilated ductal phenotype or cyst formation [8, 9, 56]. In correlation with the loss of primary cilia, we found increased proliferation of ductal cells in *Hnf1b*Δ^{duct} mutant pancreata. Moreover, this leads to duct dilatation and partial loss of apico-basal polarity of epithelial ductal cells. Some *Hnf1b*Δ^{duct} mutant ducts were devoid of primary cilia, whereas they were not dilated, strongly suggesting that duct dilatation occurs secondary to the loss of primary cilia. Furthermore, Muc1 immunostaining was still observed in some dilated ducts. We observed weaker expression of Muc1 at P25 whereas it was unchanged at P8. This strongly suggests that loss of apico-basal polarity is a consequence of duct dilatation. *Pkhd1* is also involved in the tubulogenesis and/or maintenance of duct–lumen architecture [49] and its decreased expression likely contributes to duct dilatation in *Hnf1b*Δ^{duct} mutants. Prox1 was significantly downregulated in *Hnf1b*Δ^{duct} mutants by P8 and it was previously shown that *Prox1* inactivation results in dilated pancreatic ducts and ADM. *Prox1* mutant adult pancreata uncovered features of chronic tissue damage: acinar apoptosis, macrophage infiltration, mild fibrosis, and extensive lipomatosis [21], suggesting that reduced *Prox1* expression contributes to the phenotype observed in *Hnf1b*Δ^{duct} mutants. Lineage tracing analysis showed that adipocytes of *Prox1* mutant pancreata did not originate from trans-differentiated pancreatic acinar cells [21], suggesting that this may also be the case for *Hnf1b*Δ^{duct} mutants, and rather caused by fibroblast activation [4]. Dilated ducts

were also reported in pancreata devoid of Hnf6 [56,57]. Pancreatitis was observed in *Hnf6* mutant animals [57], associated with the finding of shorter primary cilia of ductal cells [58]. We observed a decreased expression of *Hnf6* at P25 whereas it was unchanged at P8, showing that loss of Hnf6 can contribute secondarily to the phenotype. Our data further underscore the link between primary cilia and pancreatitis. Defects in cilia have been associated with a spectrum of human diseases collectively called ciliopathies [59]. Ductal cysts, polarization defects, dysplasia and fibrosis of the pancreas have been described in many ciliopathies. The absence of pancreatic cilia during mouse embryogenesis in *Kif3a* mutants or in hypomorphic Tg737 mutants (*Tg737^{orpk}*) resulted in lesions that resemble those found in patients with pancreatitis or cystic fibrosis [7–9]. However, the function of ducts and primary cilia in post-natal pancreatic tissue homeostasis was largely unknown. We show here that Hnf1b inactivation leads to loss of primary cilia and duct dilatation, Hnf1b being necessary for the expression of Pkhd1, Cys1 and Prox1 in pancreatic ducts. Our results are also of particular interest since genes we found downregulated in *Hnf1b*Δ^{duct} mutant pancreata are also linked to pancreatic neoplasia [60–62].

***Hnf1b*-inactivation in pancreatic ducts leads to neoplasia and enhances the ability of oncogenic KRAS to promote precancerous lesions.**

As cilia have the ability to physically influence the cell cycle and fine-tune signaling cascades, loss of primary cilia may promote tumorigenesis through aberrant signal transduction. Ciliogenesis was indeed found suppressed in tumor cells, including PanINs and PDAC [63]. YAP was shown to promote cell proliferation [64] and we observed an upregulation of the YAP pathway and an increased proliferation of ductal cells in *Hnf1b*Δ^{duct} mutants. Recent studies have highlighted the role of YAP in the regulation of cell proliferation during postnatal liver growth and cancer pathogenesis, increased YAP

activation was associated with hepatic cyst epithelium proliferation in autosomal recessive polycystic kidney disease (ARPKD) [24]. Moreover, YAP functions as a mechano-responsive transcriptional co-activator [25-27]. Our data suggest that mechanical stress induced by enlarging cysts stimulates YAP activation in pericystic and acinar cells. As YAP activity is necessary and sufficient for ADM and pancreatitis induction [30-32], YAP constitutes a molecular link between Hnf1b deletion in ductal cells and the non-cell autonomous effects on acinar cells. Moreover, YAP drives fibrosis by activating fibroblasts [29]. YAP transcriptional targets were progressively overexpressed from P8 to the adult stage: CTGF and Lamc2 from P8, Cyr61 by P25 and Birc5 in adults. All of them were strongly upregulated in adults, 4- to 10-fold. In correlation, a 4.5-fold increase in *CTGF* expression was observed in human chronic pancreatitis [65]. CTGF is involved in cell adhesion, cell migration, inflammation, pancreatic fibrosis, tumor growth and metastasis, and it is overexpressed in human pancreatic cancer [66]. Thus, fibrosis is likely caused by increased *CTGF* expression and this fibrotic microenvironment promotes PanINs in *Hnf1b*Δ^{duct} mutant pancreata. Moreover, LAMC2 was recently identified as a new putative pancreatic cancer biomarker [67]. EGFR, promoting ADM and PanINs [34], is also involved in ADM induction and formation of neoplastic lesions in *Hnf1b*Δ^{duct} mutants, as upregulation of *EGFR* in mutants was observed from P8, with a 2-fold increase in adults. From P25, Notch and TGF-β signaling contribute to ADM, fibrosis, activation of PSCs and PanINs development in *Hnf1b*Δ^{duct} mutants, with a 2-fold upregulation at P25 and 6-fold in adults for Notch signaling, a 4-fold upregulation at P25 and 13-fold in adults for *TGF-β1* in *Hnf1b*Δ^{duct} mutants. The selective dramatic up-regulations of Notch2 and Hey2 in *Hnf1b*Δ^{duct} mutants are in accordance with the finding that centroacinar and terminal ductal epithelial cells did not display up-regulation of *Hes1* transcripts, but did exhibit up-regulated expression of *Hey2*, consistent with an active Notch pathway [68]. Moreover,

Notch2 is expressed in ductal cells and PanIN lesions and is a central regulator of PanIN progression and malignant transformation [69]. Notch indeed regulates ADM and promotes both initiation and progression of PanINs [2,38,46]. As TGF-β was shown to trigger ADM in acinar cells [37], it would be interesting to further test the requirement of TGF-β activation to drive ADM in *Hnf1b*Δ^{duct} mutants with the use of TGF-β inhibitors. TGF-β signaling is also pivotal in driving fibrogenesis, for activation of PSC and for PanIN formation [44,70]. Thus, activation of the YAP pathway, EGFR pathway, and subsequent upregulation of the Notch and TGF-β pathways support the non-cell autonomous effects leading to ADM, PSCs activation, fibrosis and PanINs in *Hnf1b*Δ^{duct} mutants. Furthermore, we observed an increase in both the number and the grade of PanIN lesions in the pancreas of mice combining both perinatal Hnf1b inactivation in ducts and oncogenic Kras activation in mature acinar cells, showing that loss of Hnf1b promotes PanIN formation in a Kras activated context. Thus, the environnement due to Hnf1b inactivation is favorable for Kras^{G12V}-dependent carcinogenesis.

Increased risk for neoplastic conversion have also been linked to perturbations in pathways that control tissue regeneration [71]. We examined the role of Hnf1b in adult ducts in the process of tissue injury and regeneration, in the cerulein-induced acute pancreatitis model [72]. Remarkably, our findings show that *Hnf1b* inactivation in adult ductal cells is associated with impaired acinar regeneration and chronic inflammation, allowing ADM and PanIN formation in the context of tissue injury in adults. Whether this role is due to Hnf1b function in terminal ducts or centroacinar cells will require further investigations.

HNF1B **role in etiology and physiopathology of the human diseases «maturity onset diabetes of the young type 5 » (MODY5), chronic pancreatitis and**

PDAC

HNF1B heretozygous mutations are notably associated with MODY5 diabetes, pancreas exocrine dysfunction (pancreatitis with reduced fecal elastase concentration in 93% of these cases, fecal fat excretion) and pancreas structural anomalies (atrophy, cysts, calcification) [73]. Pancreatitis was surprising to observe as *Hnf1b* is not expressed in acinar cells and it was proposed that this defect might be caused by pancreas hypoplasia. The results of the present study show that pancreatitis associated with *Hnf1b* deficiency is caused by pancreatic duct alteration. Moreover, differences observed from one patient to another might be due to impaired recovery of the pancreas in adults as our results also show that *Hnf1b* deficiency leads to altered acinar regeneration following injury.

Studies have shown that downregulation of *HNF1B* is associated with cancer risk, including renal, prostate, ovarian and colorectal cancers, showing that HNF1B is a marker of these cancers and a potential tumor suppressor [74–78]. Pancreatic cancer is poorly characterized at genetic and non-genetic levels. Recent analyses suggested that reduced HNF1B activity could also be an important step in pancreatic tumorigenesis. Mutations in *HNF1B* have been identified as markers of pancreatic cancer risk loci through GWAS analyses [79-81]. In PDAC tissues and pancreatic cancer cell lines, *HNF1B* was down-regulated compared to normal pancreatic tissues and this loss of expression contributed to disease aggressiveness [62,80]. Recently, a regulatory network analysis reported that *HNF1B*, among thousand transcription factors, was the top enriched gene expressed in the normal pancreatic tissue compared to the PDAC regulatory network, identifying HNF1B as a master regulator of PDAC and its subtypes [82]. The present study is the first to demonstrate that loss of Hnf1b activity can induce pancreatitis, pancreatic neoplasia and facilitates the onset of $Kras^{G12V}$-induced PanIN. We show here some

molecular mechanisms that link *Hnf1b* dysfunction to pancreatic neoplasia and tumorigenesis. Understanding the first steps of pancreatic tumorigenesis is important and may provide new therapeutic strategies aimed at restoring a normal differentiated state. Hnf1b appears to act as a pancreatic tumor suppressor, important for the epithelial state maintenance. Hnf6, one downstream target of Hnf1b, was also proposed as a tumor suppressor [61], suggesting that maintenance of the ductal phenotype could be important in cancer prevention. Defining the molecular mechanisms underlying the initiation of pancreatic cancer is highly relevant for the development of early detection markers and of potentially novel treatments. Insight on the role of Hnf1b in pancreatic cancer development could lead to its use as a biomarker for early detection and prognosis. Reinforcing HNF1B expression may represent a novel therapeutic strategy to improve the survival of patients with PDAC, together with restoring ciliogenesis by pharmacologic means in order to improve the effectiveness of other curative options. Thus, these new insights offer potential novel therapeutic strategies.

Material and Methods

Mouse lines

The *Hnf1b* conditional knockout (Hnf1b^{tm1Lcs} denoted as Hnf1b$^{flox/flox}$) carrying LoxP sites flanking exon 4 [13] and Sox9-CreER^{T2} [14] lines have been previously described. The R26R^{YFP} line (B6.129X1-Gt(ROSA)26Sortm1(EYFP)Cos/J) from the Jackson Laboratory was used to assess recombination efficiency. We performed a conditional deletion of *Hnf1b* in pancreatic ducts by crossing the Hnf1b-floxed mouse line with the tamoxifen (TM)-inducible Sox9-CreER^{T2} line to generate Sox9-Cre^{ER};Hnf1b$^{fl/fl}$ mice referred to as

mutants. Hnf1b$^{fl/+}$ or Hnf1b$^{fl/fl}$ mice are referred to as controls. Heterozygous Sox9-CreER;Hnf1b$^{+/fl}$ mice showed no phenotype (data not shown). The Elas-tTA; TetO-Flpase; FRT-Stop-FRT Kras^{G12V} line expressed FLP recombinase under the control of the elastase promoter in a tet-off system, allowing selective expression of the KrasG12V oncoprotein in pancreatic acinar cells. Untreated mice developed PanIN lesions with a long latency [83] and were used in crossings with Sox9-CreER;Hnf1b$^{fl/fl}$ mutants with TM induction perinataly to assess if ductal Hnf1b inactivation promotes PanIN progression in concert with Kras activated in acinar cells. Elas-tTA; TetO-Flpase; Kras^{G12V} are referred to as Kras and Sox9-Cre^{ER};Hnf1b$^{fl/fl}$;Elas-tTA; TetO-Flpase; Kras^{G12V} are referred to as Mutant;Kras. Animal experiments were conducted in accordance with French and European ethical legal guidelines and the local ethical committee for animal care (Comité d'éthique en expérimentation animale Charles Darwin N°5, approval number N° 01508).

Tamoxifen treatment

Tamoxifen (Sigma-T5648) was dissolved at 25 mg/ml in corn oil and administrated intraperitoneally to mice at a dose of 7mg/40g of mouse. For postnatal inactivation, tamoxifen injections were performed on lactating females during 3 consecutive days following birth, with 1 injection per day (P1, P2, P3), allowing pups to receive tamoxifen through breast milk. Dissections were done at P8, P25, 2-months and 5-months. For adult inactivation, Tamoxifen was injected during 4 consecutive days, with 1 injection per day, to 6 or 10 weeks old mice.

Cerulein treatment

2 weeks after adult *Hnf1b* inactivation with TM injections of 10-weeks old mice, mice were injected with cerulein (Sigma-C9026), a decapeptide analogue of the pancreatic secretagogue cholecystokinin that induces acinar cell death, at a dose corresponding to 75 µg/kg. Cerulein was dissolved at 1 mg/ml in NaCl and administrated to mice at 5 µl/g by injections intraperitoneally hourly, 7 times a day, for 2 consecutive days. Pancreata were harvested at 3 different times after the first cerulein injection: just before cerulein injection at day 0 (DO), when acute pancreatitis was induced at day 3 (D3), and when the pancreas was almost fully regenerated at day 7 (D7).

Histology, Immunohistochemistry and Immunofluorescence

Dissected pancreata were fixed in 4% formaldehyde overnight and embedded in paraffin. Sections (7 µm thick) were prepared, deparaffinised and rehydrated for histological stainings. For Hematoxylin & Eosin (H&E) staining, slides were incubated with Harris solution (Sigma- HHS16) for 1 min and in Eosin (Sigma-HT110216) for 3 min. For Masson's Trichrome staining, slides were incubated with Harris for 5 min, rinsed with lithium carbonate and water, then incubated with Funchsin-Ponceau for 3 min and rinsed with acidified water and 1% phosphomolibdic acid. Slides were then stained with 1% light green for 20 min and rinsed with acidified water. For Alcian Blue staining, slides were incubated with Alcian Blue solution (pH2.5) for 30 min, prepared with Alcian Blue 8GX (Sigma-A3157) in 3% acetic acid, rinsed with water and counterstained with Nuclear Fast Red solution for 5 min. Slides were dehydrated before mounting.

Sections were processed for immunofluorescence or immunohistochemistry using a previously described protocol [16]. Briefly, epitope retrieval was performed by heating the slides in a microwave in citric acid buffer (10 mM, PH:6). Permeabilization was

performed in PBS/TritonX-100 0.3%, and sections were incubated in blocking solution (10% milk, 1% BSA 0.1% 10X Triton-X in PBS 1X or 1.5% Horse/Goat Serum in PBS 1X) before antibody staining. Nuclei were stained with DAPI (1/1000-Sigma) in the secondary antibody staining step. For signal amplification, we used a biotinylated anti-rabbit or anti-goat antibody before incubating with Steptavidin-Alexa594 or Steptavidin-Alexa488. Epitope retrieval for CTGF immunohistochemistry was performed by heating slides in a pressure cooker for 15 minutes. Slides were then incubated in 3% H2O2 before blocking to eliminate endogenous peroxidase activity. For all other immunohistochemistry experiments, slides were incubated in 1% H2O2/50% methanol solution before blocking to eliminate endogenous peroxidase activity. The VECTASTAIN peroxidase ABC system (Vector) was used for Sox9, F4/80, vimentin, CTGF, Hey2, P-AKT, P-SMAD2 and Claudin18 immunostainings. Nuclei were counterstained with Hematoxylin. Primary antibodies are listed in Table 1. Images were acquired using Zeiss Axio Observer.Z1 microscope with apotome. For histology, immunofluorescence and immunohistochemistry, at least 2 sections per pancreas and at least 3 different pancreases of each genotype were analyzed.

Quantification of recombined GFP+ ducts, ciliated ductal cells, duct area, proliferation & apoptosis, and PanINs

Quantification of GFP+ ducts in mutants was performed with GFP/Hnf1b immunostainings. More than 2500 GFP+ cells and 500 Hnf1b+ cells were counted (n=3). Quantification of ciliated ductal cells at P8 was performed by counting Sox9+ cells with the cilium stained with Acetylated Tubulin. Almost 500 cells were counted for controls and more than 1,000 cells for mutants (Control, n=7; Mutant, n=11). Quantifications of Sox9+ and Amylase+ cells at P8 were performed with at least 2 sections per pancreas

(Control, n=4; Mutant, n=4). More than 15,000 Sox9+ and 22,000 Amylase+ cells were counted for each genotype. The numbers of Sox9+ and Amylase+ cells per mm^2 were obtained by dividing the numbers of Sox9+ and Amylase+ cells by the corresponding cross-sectional areas.

Proliferation of ductal and acinar cells was determined by immunolabeling with Phospho-histone H3 (PPH3) and Sox9 or Amylase antibodies respectively. Positive cells were scored from at least 3 non-overlapping fields for each section at 10X magnification. The percentages of PPH3 positive cells were calculated by dividing the number of ductal or acinar cells labeled with PPH3 by the total number of cells expressing Sox9 or Amylase. Quantification was performed with at least 2 sections per pancreas (Control, n=4; Mutant, n=4).

Acinar cell apoptosis was determined with a Terminal deoxynucleotidyltransferase-mediated dUTP-biotin nick end labeling (TUNEL) analysis, performed using an in situ cell death detection kit (Roche Diagnostics) and followed by amylase immunostaining. Apoptosis was quantified by counting the number of labelled nuclei. The percentage of TUNEL-positive cells was calculated by dividing the number of TUNEL+/Amylase+ cells by the total number of Amylase+ acinar cells. Quantification was performed with 3 sections per pancreas (Control, n=4; Mutant, n=4). More than 100 TUNEL stained acinar cells were counted in controls and more than 800 in mutants.

All countings were performed with Adobe Photoshop CS4.

Quantification of the % of remaining acini, adipocytes, fibrosis/infiltrates, ADM and PanIN was performed on histological sections of mutant pancreata (n=6) with Image J/Fiji software.

Quantification of the lesion surface in Mutant;Kras compared to Kras and Mutants was performed by measuring the surface of the lesions positive for Alcian Blue divided by

the total surface of the pancreatic area in μm^2. The results are given in percentage. Each image of the most representative section per sample was acquired by a macro-apotome Zeiss Axiozoomer and the surfaces were quantified by the Zen software. The total number of lesions was counted on each image acquired by the macro-apotome for each sample and was reported to the total surface of the pancreatic area. The results are given as the number of lesion per cm^2. The size of each lesion was also quantified in μm^2. Mutants n=5, Kras n=4, Mutant;Kras n= 3.

Values are shown as mean+s.e.m.

RNA extraction, Reverse-Transcription and quantitative PCR (RT-qPCR)

Total RNA from adult pancreas was isolated using the RNeasy Mini-kit (Qiagen) and reverse transcribed using the Superscript RT II Kit with random hexamers (Invitrogen). qPCR was performed using a SYBR Green master mix (Eurobiogreen QPCR Mix, Hi-ROX, Eurobio). Primer sequences are provided in Table 2. The method of relative quantification was used to calculate expression levels, normalized to cyclophilin A and relative to wild-type cDNA from E15.5 pancreata. Values are shown as mean+s.e.m.

Statistical analysis

Statistical significance was determined using Student's t-test or the non-parametric Mann-Whitney's U test when appropriate. Statistical analyses were carried out with GraphPad Prism 6.0 (GraphPad Software, Inc, La Jolla, CA, USA). Differences were considered significant for $P< 0.05$. (NS, not significant; *P<0.05; **P<0.01; ***P<0.001).

Acknowledgements

We thank Edouard Manzoni and Edwige Declerc for technical help, mouse facilities of the UMR722-IBPS for animal care, the imaging platform of the IBPS for image acquisitions with the macro-apotome and Sophie Gournet for illustrations. We also thank P. Jacquemin and F. Lemaigre (De Duve Institute, Belgium) for Hnf6 antibody and Christine Vesque for critical reading of the manuscript.

References

1. Pinho AV, Chantrill L, Rooman I. Chronic pancreatitis: a path to pancreatic cancer. Cancer Lett 2014;345:203–209.

2. De La O J-P, Emerson LL, Goodman JL, Froebe SC, Illum BE, Curtis AB, Murtaugh LC. Notch and Kras reprogram pancreatic acinar cells to ductal intraepithelial neoplasia. Proc Natl Acad Sci USA 2008;105:18907–18912.

3. Guerra C, Schuhmacher AJ, Cañamero M, Grippo PJ, Verdaguer L, Pérez-Gallego L, Dubus P, Sandgren EP, Barbacid M. Chronic pancreatitis is essential for induction of pancreatic ductal adenocarcinoma by K-Ras oncogenes in adult mice. Cancer Cell 2007;11:291–302.

4. Kleeff J, Whitcomb DC, Shimosegawa T, Esposito I, Lerch MM, Gress T, Mayerle J, Drewes AM, Rebours V, Akisik F, Muñoz JED, Neoptolemos JP. Chronic pancreatitis. Nat Rev Dis Primers 2017;3:17060.

5. Reichert M, Rustgi AK. Pancreatic ductal cells in development, regeneration, and neoplasia. J Clin Invest 2011;121:4572–4578.

6. Larsen HL, Grapin-Botton A. The molecular and morphogenetic basis of pancreas organogenesis. Semin Cell Dev Biol 2017;66:51–68.

7. Cano DA, Murcia NS, Pazour GJ, Hebrok M. Orpk mouse model of polycystic kidney disease reveals essential role of primary cilia in pancreatic tissue organization. Development 2004;131:3457–3467.

8. Cano DA, Sekine S, Hebrok M. Primary cilia deletion in pancreatic epithelial cells results in cyst formation and pancreatitis. Gastroenterology 2006;131:1856–1869.

9. Zhang Q, Davenport JR, Croyle MJ, Haycraft CJ, Yoder BK. Disruption of IFT results in both exocrine and endocrine abnormalities in the pancreas of Tg737(orpk) mutant mice. Lab Invest 2005;85:45–64.

10. Lodh S, O'Hare EA, Zaghloul NA. Primary cilia in pancreatic development and disease. Birth Defects Res C Embryo Today 2014;102:139–158.

11. Maestro MA, Boj SF, Luco RF, Pierreux CE, Cabedo J, Servitja JM, German MS, Rousseau GG, Lemaigre FP, Ferrer J. Hnf6 and Tcf2 (MODY5) are linked in a gene network operating in a precursor cell domain of the embryonic pancreas. Hum Mol Genet 2003;12:3307–3314.

12. Solar M, Cardalda C, Houbracken I, Martín M, Maestro MA, De Medts N, Xu X, Grau V, Heimberg H, Bouwens L, Ferrer J. Pancreatic exocrine duct cells give rise to insulin-producing beta cells during embryogenesis but not after birth. Dev Cell 2009;17:849–860.

13. De Vas MG, Kopp JL, Heliot C, Sander M, Cereghini S, Haumaitre C. Hnf1b controls pancreas morphogenesis and the generation of Ngn3+ endocrine progenitors. Development 2015;142:871–882.

14. Kopp JL, Dubois CL, Schaffer AE, Hao E, Shih HP, Seymour PA, Ma J, Sander M. Sox9+ ductal cells are multipotent progenitors throughout development but do not produce new endocrine cells in the normal or injured adult pancreas. Development 2011;138:653–665.

15. Houbracken I, Bouwens L. Acinar cells in the neonatal pancreas grow by self-duplication and not by neogenesis from duct cells. Sci Rep 2017;7:12643.

16. Haumaitre C, Barbacci E, Jenny M, Ott MO, Gradwohl G, Cereghini S. Lack of TCF2/vHNF1 in mice leads to pancreas agenesis. Proc Natl Acad Sci USA 2005;102:1490–1495.

17. Gresh L, Fischer E, Reimann A, Tanguy M, Garbay S, Shao X, Hiesberger T, Fiette L, Igarashi P, Yaniv M, Pontoglio M. A transcriptional network in polycystic kidney disease. EMBO J 2004;23:1657–1668.

18. Masyuk TV, Huang BQ, Ward CJ, Masyuk AI, Yuan D, Splinter PL, Punyashthiti R, Ritman EL, Torres VE, Harris PC, LaRusso NF. Defects in cholangiocyte fibrocystin expression and ciliary structure in the PCK rat. Gastroenterology 2003;125:1303–1310.

19. Raynaud P, Tate J, Callens C, Cordi S, Vandersmissen P, Carpentier R, Sempoux C, Devuyst O, Pierreux CE, Courtoy P, Dahan K, Delbecque K, Lepreux S, Pontoglio M, Guay-Woodford LM, Lemaigre FP. A classification of ductal plate malformations

based on distinct pathogenic mechanisms of biliary dysmorphogenesis. Hepatology 2011;53:1959–1966.

20. Kilic G, Wang J, Sosa-Pineda B. Osteopontin is a novel marker of pancreatic ductal tissues and of undifferentiated pancreatic precursors in mice. Dev Dyn 2006;235:1659–1667.

21. Westmoreland JJ, Kilic G, Sartain C, Sirma S, Blain J, Rehg J, Harvey N, Sosa-Pineda B. Pancreas-specific deletion of Prox1 affects development and disrupts homeostasis of the exocrine pancreas. Gastroenterology 2012;142:999–1009.e6.

22. Kobayashi T, Dynlacht BD. Regulating the transition from centriole to basal body. The Journal of Cell Biology 2011;193:435–444.

23. Basten SG, Giles RH. Functional aspects of primary cilia in signaling, cell cycle and tumorigenesis. Cilia 2013;2:6.

24. Jiang L, Sun L, Edwards G, Manley M Jr, Wallace DP, Septer S, Manohar C, Pritchard MT, Apte U. Increased YAP activation is associated with hepatic cyst epithelial cell proliferation in ARPKD/CHF. Gene Expr 2017;17:313–326.

25. Halder G, Dupont S, Piccolo S. Transduction of mechanical and cytoskeletal cues by YAP and TAZ. Nat Rev Mol Cell Biol 2012;13:591–600.

26. Low BC, Pan CQ, Shivashankar GV, Bershadsky A, Sudol M, Sheetz M. YAP/TAZ as mechanosensors and mechanotransducers in regulating organ size and tumor growth. FEBS Lett 2014;588:2663–2670.

27. Panciera T, Azzolin L, Cordenonsi M, Piccolo S. Mechanobiology of YAP and TAZ in physiology and disease. Nat Rev Mol Cell Biol. 2017;18:758-770.

28. Pi L, Robinson PM, Jorgensen M, Oh SH, Brown AR, Weinreb PH, Trinh TL, Yianni P, Liu C, Leask A, Violette SM, Scott EW, Schultz GS, Petersen BE. Connective tissue growth factor and integrin αvβ6: a new pair of regulators critical for ductular reaction and biliary fibrosis in mice. Hepatology 2015;61:678–691.

29. Liu F, Lagares D, Choi KM, Stopfer L, Marinković A, Vrbanac V, Probst CK, Hiemer SE, Sisson TH, Horowitz JC, Rosas IO, Fredenburgh LE, Feghali-Bostwick C, Varelas X, Tager AM, Tschumperlin DJ. Mechanosignaling through YAP and TAZ drives fibroblast activation and fibrosis. Am J Physiol Lung Cell Mol Physiol. 2015;308:L344-57.

30. Gao T, Zhou D, Yang C, Singh T, Penzo-Méndez A, Maddipati R, Tzatsos A, Bardeesy N, Avruch J, Stanger BZ. Hippo signaling regulates differentiation and maintenance in the exocrine pancreas. Gastroenterology. 2013;144:1543-53, 1553.e1.

31. Morvaridi S, Dhall D, Greene MI, Pandol SJ, Wang Q. Role of YAP and TAZ in pancreatic ductal adenocarcinoma and in stellate cells associated with cancer and chronic pancreatitis. Sci Rep. 2015;5:16759.

32. Gruber R, Panayiotou R, Nye E, Spencer-Dene B, Stamp G, Behrens A. YAP1 and TAZ control pancreatic cancer initiation in mice by direct up-regulation of JAK–STAT3 signaling. Gastroenterology. 2016; 151: 526–539.

33. Means AL, Meszoely IM, Suzuki K, Miyamoto Y, Rustgi AK, Coffey RJ Jr, Wright CV, Stoffers DA, Leach SD. Pancreatic epithelial plasticity mediated by acinar cell

transdifferentiation and generation of nestin-positive intermediates. Development 2005;132:3767–3776.

34. Navas C, Hernández-Porras I, Schuhmacher AJ, Sibilia M, Guerra C, Barbacid M. EGF receptor signaling is essential for k-ras oncogene-driven pancreatic ductal adenocarcinoma. Cancer Cell 2012;22:318–330.

35. Liu J, Akanuma N, Liu C, Naji A, Halff GA, Washburn WK, Sun L, Wang P. TGF-β1 promotes acinar to ductal metaplasia of human pancreatic acinar cells. Sci Rep 2016;6:30904.

36. Prévot P-P, Simion A, Grimont A, Colletti M, Khalaileh A, Van den Steen G, Sempoux C, Xu X, Roelants V, Hald J, Bertrand L, Heimberg H, Konieczny SF, Dor Y, Lemaigre FP, Jacquemin P. Role of the ductal transcription factors HNF6 and Sox9 in pancreatic acinar-to-ductal metaplasia. Gut 2012;61:1723–1732.

37. Chuvin N, Vincent DF, Pommier RM, Alcaraz LB, Gout J, Caligaris C, Yacoub K, Cardot V, Roger E, Kaniewski B, Martel S, Cintas C, Goddard-Léon S, Colombe A, Valantin J, Gadot N, Servoz E, Morton J, Goddard I, Couvelard A, Rebours V, Guillermet J, Sansom OJ, Treilleux I, Valcourt U, Sentis S, Dubus P, Bartholin L. Acinar-to-Ductal Metaplasia Induced by Transforming Growth Factor Beta Facilitates KRASG12D-driven Pancreatic Tumorigenesis. Cell Mol Gastroenterol Hepatol. 2017;4:263-282.

38. Miyamoto Y, Maitra A, Ghosh B, Zechner U, Argani P, Iacobuzio-Donahue CA, Sriuranpong V, Iso T, Meszoely IM, Wolfe MS, Hruban RH, Ball DW, Schmid RM, Leach SD. Notch mediates TGFα-induced changes in epithelial differentiation during pancreatic tumorigenesis. Cancer Cell 2003;3:565–576.

39. Lammert E, Brown J, Melton DA. Notch gene expression during pancreatic organogenesis. Mechanisms of Development 2000;94:199–203.

40. Bhanot U, Köhntop R, Hasel C, Möller P. Evidence of Notch pathway activation in the ectatic ducts of chronic pancreatitis. J Pathol 2008;214:312–319.

41. Mallo GV, Fiedler F, Calvo EL, Ortiz EM, Vasseur S, Keim V, Morisset J, Iovanna JL. Cloning and Expression of the Rat p8 cDNA, a New Gene Activated in Pancreas during the Acute Phase of Pancreatitis, Pancreatic Development, and Regeneration, and Which Promotes Cellular Growth. J Biol Chem 1997;272:32360–32369.

42. Siersbaek R, Nielsen R, Mandrup S. PPARgamma in adipocyte differentiation and metabolism--novel insights from genome-wide studies. FEBS Lett 2010;584:3242–3249.

43. Apte MV, Pirola RC, Wilson JS. Pancreatic stellate cells: a starring role in normal and diseased pancreas. Front Physiol 2012;3:344.

44. Korc M. Pancreatic cancer-associated stroma production. Am J Surg 2007;194:S84–86.

45. Haque I, Mehta S, Majumder M, Dhar K, De A, McGregor D, Van Veldhuizen PJ, Banerjee SK, Banerjee S. Cyr61/CCN1 signaling is critical for epithelial-mesenchymal transition and stemness and promotes pancreatic carcinogenesis. Mol Cancer 2011;10:8.

46. Leach SD. Epithelial differentiation in pancreatic development and neoplasia: new niches for nestin and Notch. J Clin Gastroenterol 2005;39:S78–82.

47. Criscimanna A, Speicher JA, Houshmand G, Shiota C, Prasadan K, Ji B, Logsdon CD, Gittes GK, Esni F. Duct cells contribute to regeneration of endocrine and acinar cells following pancreatic damage in adult mice. Gastroenterology 2011;141:1451–1462, 1462.e1–6.

48. Murtaugh LC, Keefe MD. Regeneration and repair of the exocrine pancreas. Annu Rev Physiol 2015;77:229–249.

49. Zhang M-Z, Mai W, Li C, Cho SY, Hao C, Moeckel G, Zhao R, Kim I, Wang J, Xiong H, Wang H, Sato Y, Wu Y, Nakanuma Y, Lilova M, Pei Y, Harris RC, Li S, Coffey RJ, Sun L, Wu D, Chen XZ, Breyer MD, Zhao ZJ, McKanna JA, Wu G. PKHD1 protein encoded by the gene for autosomal recessive polycystic kidney disease associates with basal bodies and primary cilia in renal epithelial cells. PNAS 2004;101:2311–2316.

50. Kim I, Fu Y, Hui K, Moeckel G, Mai W, Li C, Liang D, Zhao P, Ma J, Chen XZ, George AL Jr, Coffey RJ, Feng ZP, Wu G. Fibrocystin/polyductin modulates renal tubular formation by regulating polycystin-2 expression and function. J Am Soc Nephrol 2008;19:455–468.

51. Dong F, Chen Q-Q, Zhuang Z-H, He QL, Wang FQ, Liu QC, Liu HK, Wang Y. Multiple gene mutations in patients with type 2 autoimmune pancreatitis and its clinical features. Cent Eur J Immunol 2014;39:77–82.

52. Hou X, Mrug M, Yoder BK, Lefkowitz EJ, Kremmidiotis G, D'Eustachio P, Beier DR, Guay-Woodford LM. Cystin, a novel cilia-associated protein, is disrupted in the cpk mouse model of polycystic kidney disease. J Clin Invest 2002;109:533–540.

53. Pazour GJ, Dickert BL, Vucica Y, Seeley ES, Rosenbaum JL, Witman GB, Cole DG. Chlamydomonas IFT88 and its mouse homologue, polycystic kidney disease gene tg737, are required for assembly of cilia and flagella. J Cell Biol 2000;151:709–718.

54. Oh EC, Katsanis N. Cilia in vertebrate development and disease. Development 2012;139:443–448.

55. Pugacheva EN, Jablonski SA, Hartman TR, Henske EP, Golemis EA. HEF1-dependent Aurora A activation induces disassembly of the primary cilium. Cell 2007;129:1351–1363.

56. Pierreux CE, Poll AV, Kemp CR, Clotman F, Maestro MA, Cordi S, Ferrer J, Leyns L, Rousseau GG, Lemaigre FP. The transcription factor hepatocyte nuclear factor-6 controls the development of pancreatic ducts in the mouse. Gastroenterology 2006;130:532–541.

57. Zhang H, Ables ET, Pope CF, Washington MK, Hipkens S, Means AL, Path G, Seufert J, Costa RH, Leiter AB, Magnuson MA, Gannon M. Multiple, temporal-specific roles for HNF6 in pancreatic endocrine and ductal differentiation. Mech Dev 2009;126:958–973.

58. Augereau C, Collet L, Vargiu P, Guerra C, Ortega S, Lemaigre FP, Jacquemin P. Chronic pancreatitis and lipomatosis are associated with defective function of ciliary genes in pancreatic ductal cells. Hum Mol Genet 2016.

59. Badano JL, Mitsuma N, Beales PL, Katsanis N.The ciliopathies: an emerging class of human genetic disorders. Annu Rev Genomics Hum Genet 2006;7:125–148.

ACCEPTED MANUSCRIPT

60. Jiang X, Zhang W, Kayed H, Zheng P, Giese NA, Friess H, Kleeff J. Loss of ONECUT1 expression in human pancreatic cancer cells. Oncol Rep 2008;19:157–163.

61. Pekala KR, Ma X, Kropp PA, Petersen CP1, Hudgens CW, Chung CH, Shi C, Merchant NB, Maitra A, Means AL, Gannon MA. Loss of HNF6 expression correlates with human pancreatic cancer progression. Lab Invest 2014;94:517–527.

62. Drosos Y, Neale G, Ye J, Paul L, Kuliyev E, Maitra A, Means AL, Washington MK, Rehg J, Finkelstein DB, Sosa-Pineda B. Prox1-Heterozygosis Sensitizes the Pancreas to Oncogenic Kras-Induced Neoplastic Transformation. Neoplasia 2016;18:172–184.

63. Seeley ES, Carrière C, Goetze T, Longnecker DS, Korc M. Pancreatic cancer and precursor pancreatic intraepithelial neoplasia lesions are devoid of primary cilia. Cancer Res 2009;69:422–430.

64. Zhao B, Tumaneng K, Guan K-L. The Hippo pathway in organ size control, tissue regeneration and stem cell self-renewal. Nat Cell Biol 2011;13:877–883.

65. di Mola FF, Friess H, Martignoni ME, Di Sebastiano P, Zimmermann A, Innocenti P, Graber H, Gold LI, Korc M, Büchler MW. Connective tissue growth factor is a regulator for fibrosis in human chronic pancreatitis. Ann Surg 1999;230:63–71.

66. Charrier A, Brigstock DR. Regulation of pancreatic function by connective tissue growth factor (CTGF, CCN2). Cytokine Growth Factor Rev. 2013;24:59-68.

67. Kosanam H, Prassas I, Chrystoja CC, Soleas I, Chan A, Dimitromanolakis A, Blasutig IM, Rückert F, Gruetzmann R, Pilarsky C, Maekawa M, Brand R, Diamandis EP. Laminin, gamma 2 (LAMC2): a promising new putative pancreatic cancer

ACCEPTED MANUSCRIPT

biomarker identified by proteomic analysis of pancreatic adenocarcinoma tissues. Mol Cell Proteomics 2013;12:2820–2832.

68. Rovira M, Scott S-G, Liss AS, Jensen J, Thayer SP, Leach SD. Isolation and characterization of centroacinar/terminal ductal progenitor cells in adult mouse pancreas. Proc Natl Acad Sci USA 2010;107:75–80.

69. Mazur PK, Einwächter H, Lee M, Sipos B, Nakhai H, Rad R, Zimber-Strobl U, Strobl LJ, Radtke F, Klöppel G, Schmid RM, Siveke JT. Notch2 is required for progression of pancreatic intraepithelial neoplasia and development of pancreatic ductal adenocarcinoma. Proc Natl Acad Sci USA 2010;107:13438–13443.

70. Friess H, Lu Z, Riesle E, Uhl W, Bründler AM, Horvath L, Gold LI, Korc M, Büchler MW. Enhanced expression of TGF-betas and their receptors in human acute pancreatitis. Ann Surg 1998;227:95–104.

71. Stanger BZ, Hebrok M. Control of cell identity in pancreas development and regeneration. Gastroenterology 2013;144:1170–1179.

72. Lugea A, Nan L, French SW, Bezerra JA, Gukovskaya AS, Pandol SJ. Pancreas recovery following cerulein-induced pancreatitis is impaired in plasminogen-deficient mice. Gastroenterology 2006;131:885–899.

73. Chen Y-Z, Gao Q, Zhao X-Z, Chen YZ, Bennett CL, Xiong XS, Mei CL, Shi YQ, Chen XM. Systematic review of TCF2 anomalies in renal cysts and diabetes syndrome/maturity onset diabetes of the young type 5. Chin Med J 2010;123:3326–33.

74. Grisanzio C, Werner L, Takeda D, Awoyemi BC, Pomerantz MM, Yamada H, Sooriakumaran P, Robinson BD, Leung R, Schinzel AC, Mills I, Ross-Adams H, Neal DE, Kido M, Yamamoto T, Petrozziello G, Stack EC, Lis R, Kantoff PW, Loda M, Sartor O, Egawa S, Tewari AK, Hahn WC, Freedman ML. Genetic and functional analyses implicate the NUDT11, HNF1B, and SLC22A3 genes in prostate cancer pathogenesis. Proc Natl Acad Sci USA 2012;109:11252–11257.

75. Cuff J, Salari K, Clarke N, Esheba GE, Forster AD, Huang S, West RB, Higgins JP, Longacre TA, Pollack JR. Integrative bioinformatics links HNF1B with clear cell carcinoma and tumor-associated thrombosis. PLoS ONE 2013;8:e74562.

76. Buchner A, Castro M, Hennig A, Popp T, Assmann G, Stief CG, Zimmermann W.Downregulation of HNF-1B in renal cell carcinoma is associated with tumor progression and poor prognosis. Urology 2010;76:507.e6–11.

77. Terasawa K, Toyota M, Sagae S, Ogi K, Suzuki H, Sonoda T, Akino K, Maruyama R, Nishikawa N, Imai K, Shinomura Y, Saito T, Tokino T. Epigenetic inactivation of TCF2 in ovarian cancer and various cancer cell lines. Br J Cancer 2006;94:914–921.

78. Silva TD, Vidigal VM, Felipe AV, DE Lima JM, Neto RA, Saad SS, Forones NM. DNA methylation as an epigenetic biomarker in colorectal cancer. Oncol Lett 2013;6:1687–1692.

79. Li D, Duell EJ, Yu K, Risch HA, Olson SH, Kooperberg C, Wolpin BM, Jiao L, Dong X, Wheeler B, Arslan AA, Bueno-de-Mesquita HB, Fuchs CS, Gallinger S, Gross M, Hartge P, Hoover RN, Holly EA, Jacobs EJ, Klein AP, LaCroix A, Mandelson MT, Petersen G, Zheng W, Agalliu I, Albanes D, Boutron-Ruault MC, Bracci PM, Buring JE, Canzian F, Chang K, Chanock SJ, Cotterchio M, Gaziano JM, Giovannucci EL, Goggins

M, Hallmans G, Hankinson SE, Hoffman Bolton JA, Hunter DJ, Hutchinson A, Jacobs KB, Jenab M, Khaw KT, Kraft P, Krogh V, Kurtz RC, McWilliams RR, Mendelsohn JB, Patel AV, Rabe KG, Riboli E, Shu XO, Tjønneland A, Tobias GS, Trichopoulos D, Virtamo J, Visvanathan K, Watters J, Yu H, Zeleniuch-Jacquotte A, Amundadottir L, Stolzenberg-Solomon RZ. Pathway analysis of genome-wide association study data highlights pancreatic development genes as susceptibility factors for pancreatic cancer. Carcinogenesis 2012;33:1384–1390.

80. Hoskins JW, Jia J, Flandez M, Parikh H, Xiao W, Collins I, Emmanuel MA, Ibrahim A, Powell J, Zhang L, Malats N, Bamlet WR, Petersen GM, Real FX, Amundadottir LT. Transcriptome analysis of pancreatic cancer reveals a tumor suppressor function for HNF1A. Carcinogenesis 2014;35:2670-8.

81. Klein AP,2, Wolpin BM, Risch HA, Stolzenberg-Solomon RZ, Mocci E, Zhang M, Canzian F, Childs EJ, Hoskins JW, Jermusyk A, Zhong J, Chen F, Albanes D, Andreotti G, Arslan AA, Babic A, Bamlet WR, Beane-Freeman L, Berndt SI, Blackford A, Borges M, Borgida A, Bracci PM, Brais L, Brennan P, Brenner H, Bueno-de-Mesquita B, Buring J, Campa D, Capurso G, Cavestro GM, Chaffee KG, Chung CC, Cleary S, Cotterchio M, Dijk F, Duell EJ, Foretova L, Fuchs C, Funel N, Gallinger S, M Gaziano JM, Gazouli M, Giles GG, Giovannucci E, Goggins M, Goodman GE, Goodman PJ, Hackert T, Haiman C, Hartge P, Hasan M, Hegyi P, Helzlsouer KJ, Herman J, Holcatova I, Holly EA, Hoover R, Hung RJ, Jacobs EJ, Jamroziak K, Janout V, Kaaks R, Khaw KT, Klein EA, Kogevinas M, Kooperberg C, Kulke MH, Kupcinskas J, Kurtz RJ, Laheru D, Landi S, Lawlor RT, Lee IM, LeMarchand L, Lu L, Malats N, Mambrini A, Mannisto S, Milne RL, Mohelníková-Duchoňová B, Neale RE, Neoptolemos JP, Oberg AL, Olson SH, Orlow I, Pasquali C, Patel AV, Peters U, Pezzilli R, Porta M, Real FX,

Rothman N, Scelo G, Sesso HD, Severi G, Shu XO, Silverman D, Smith JP, Soucek P, Sund M, Talar-Wojnarowska R, Tavano F, Thornquist MD, Tobias GS, Van Den Eeden SK, Vashist Y, Visvanathan K, Vodicka P, Wactawski-Wende J, Wang Z, Wentzensen N, White E, Yu H, Yu K, Zeleniuch-Jacquotte A, Zheng W, Kraft P, Li D, Chanock S, Obazee O, Petersen GM, Amundadottir LT.Genome-wide meta-analysis identifies five new susceptibility loci for pancreatic cancer. Nat Commun. 2018;9:556.

82. Janky R, Binda MM, Allemeersch J, Van den Broeck A, Govaere O, Swinnen JV, Roskams T, Aerts S, Topal B. Prognostic relevance of molecular subtypes and master regulators in pancreatic ductal adenocarcinoma. BMC Cancer 2016;16:632.

83. Blasco MT, Navas C, Martín-Serrano G, Graña-Castro O, Lechuga CG, Martín-Díaz L, Djurec M, Li J, Morales-Cacho L, Esteban-Burgos L, Perales-Patón J, Bousquet-Mur E, Castellano E, Jacob HKC, Cabras L, Musteanu M, Drosten M, Ortega S, Mulero F, Sainz B Jr, Dusetti N, Iovanna J, Sánchez-Bueno F, Hidalgo M, Khiabanian H, Rabadán R, Al-Shahrour F, Guerra C, Barbacid M. Complete Regression of Advanced Pancreatic Ductal Adenocarcinomas upon Combined Inhibition of EGFR and C-RAF. Cancer Cell. 2019;35:573-587.e6.

ACCEPTED MANUSCRIPT

Figure legends

Figure 1. Ductal deletion of *Hnf1b* leads to loss of primary cilia, increased ductal cell proliferation, dilatation, and alteration of ductal cell polarity at P8. (A) Analysis of *Hnf1b* inactivation efficiency by qRT-PCR. (B, C) Hnf1b (red) and GFP (green) immunostaining. Hnf1b+ ductal cells are observed in controls and recombination is monitored by GFP+ cells in Sox9-Cre^{ER};Hnf1b$^{fl/fl}$;R26R$^{YFP/+}$ mutant pancreata. (D) Quantification of GFP+ recombined ductal cells in Sox9-Cre^{ER};Hnf1b$^{fl/fl}$;R26R$^{YFP/+}$ mutant pancreata. (E) qRT-PCR of ductal and cystic-disease genes. (F, G) Sox9 (green) and acetylated α-Tubulin (Ac-Tub, red) immunostaining. (H, I) Muc1 (green) and Arl13b (red) immunostaining. Mutant ductal epithelial cells stained with Sox9 and Muc1 are devoid of primary cilia, stained for Ac-Tub (G') and Arl13b (I'). (J) Quantification of ciliated ductal cells. (K, L, M) GFP and Ac-Tub immunostaining showing primary cilia loss in recombinant ductal cells from dilated (M') and non-dilated (L') ducts. (N, O) Phospho-histone H3 (PHH3, red) and Sox9 (green) immunostaining. (P, Q) Quantification of ductal Sox9^{+} cell proliferation and quantification of the number Sox9^{+} cells per area. Arrows indicate mitotic Sox9^{+} cells. (R, S) H&E staining. (T, U) Sox9 (brown) immunohistochemistry. (V, W) PKCz (green) and β-Cat (red) immunostaining. (W) Asterisk shows dilated duct with loss of PKCz apical staining. PKCz apical staining is maintained in non-dilated duct (W') but lost in dilated ducts (W''). (X, Y) Mucin1 (Muc1, green) and β-catenin (β-Cat, red) immunostaining. (Y, Y') Arrows show disruption of Muc1 staining in parts of mutant dilated ducts. (Z-AA) Spp1 (red) and Amylase (green) immunostaining. Loss of the apical ductal marker Spp1 is observed in mutants (AA'). Nuclei are stained with DAPI (blue). Scale bars: (B-C, N-O, R-U) 50 μm; (X-Y) 30 μm; (F-I,

K-M, V-W, Z-AA) 10 µm. Control, n=7; Mutant, n=7 for RT-qPCR and Control, n≥3; Mutant, n≥3 for immunostainings. *P<0.05; **P<0.01; ***P<0.001.

Figure 2. Ductal deletion of *Hnf1b* leads to upregulation of the YAP pathway at P8. (A, B) Sox9 (green) and α-smooth muscle actin (SMA, red) immunostaining. SMA staining is observed in smooth muscle cells in vessel walls in controls (A), whereas SMA is ectopically activated in periductal cells in mutants (B). (C, D) YAP (red) and Sox9 (green) immunostaining. (E, F) YAP (red) and Amylase (green) immunostaining. Nuclear YAP immunostaining is ectopically localized in periductal and acinar cells in mutants (D, F). (G) RT-qPCR analysis of YAP transcriptional targets. (H-M) YAP (red) and Sox9 (green) immunostaining. Merged images show YAP/Sox9 colocalisation in ductal cells in controls (J') and mutants (M'). (N-S) YAP (red) and Amylase (green) immunostaining. No YAP/Amylase colocalisation is present in controls (P'), whereas Amylase+ cells show YAP+ nuclear staining in mutants (S'). Nuclei are stained with DAPI (blue). Scale bars: (A-F) 50µm; (H-S) 20 µm. ***P*<0.01. Control, n=7; Mutant, n=7 for RT-qPCR and Control, n≥3; Mutant, n≥3 for immunostainings.

Figure 3. Ductal deletion of *Hnf1b* induces pancreatic fibrosis and loss of acinar cells by P8. (A, B) Masson's Trichrome staining show collagen deposition in green in mutants. (C) qRT-PCR analysis of acinar markers. (D) Number of Amylase$^+$ cells per area. (E) qRT-PCR of *EGFR* and *TGF-β1*. (F, G) Phospho-histone H3 (PHH3, red) and Amylase (green) immunostaining. Arrows indicate mitotic Amylase$^+$ cells. (H) Quantification of acinar cell proliferation (Amylase+ PHH3+/Amylase+ cells). (I, J) TUNEL assay (green) and Amylase (red) immunostaining. Arrows indicate apoptotic Amylase$^+$ cells. Nuclei are stained with DAPI (blue). (K) Quantification of acinar cell apoptosis. Scale bars: 50 µm.

Control, n=4; Mutant, n=4 for quantification of immunostainings, and Control, n=7; Mutant, n=7 for RT-qPCR. **P<0.01; ***P<0.001.

Figure 4. Ductal deletion of *Hnf1b* leads to ADM and lipomatosis at P25. (A, B) H&E staining. Arrows show acini with increased lumen size in mutants, feature of ADM. (C, D) Amylase (green) and Hnf1b (red) immunostaining. (E, F) Amylase (green) and Sox9 (red) immunostaining. (G-H) Amylase (green) and Hnf6 (red) immunostaining. Arrows show Amylase+ cells with nuclear Hnf6+ staining, characteristic of ADM in mutants. (I) RTq-PCR of acinar markers. (J) RTq-PCR of *Hnf6*, *Muc1*, *Sox9*. (K, L) Muc1 (green) and β-Cat (red) immunostaining. Muc1 staining is lost at the apical surface of ductal cells in mutants. (M, N) Amylase (green) and PanCK (red) immunostaining. PanCK localisation is expanded in acinar cells of mutants (N'). (O, P) FABP4 immunostaining shows adipocytes in mutants. (Q) RT-qPCR of YAP transcriptional targets (R) RT-qPCR of Notch signaling components. (S) RT-qPCR of *TGF-β1* and *P8/NuPr1.* Scale bars: 50 μm. Nuclei are stained with DAPI (blue). Control, n≥3; Mutant, n≥3 for immunostainings and Control, n=7; Mutant, n=8 for RT-qPCR. *P<0.05; **P<0.01; ***P<0.001.

Figure 5. Ductal deletion of *Hnf1b* leads to chronic pancreatitis at 2 months. (A) Pancreas weight and relative pancreas weight/body weight of 2-months old mice (Control, n=17; Mutant, n=11). (B-F) H&E staining. Mutant pancreata display dramatic loss of acinar tissue (C) and ADM (E, F). (G, H) Amylase (green) and Sox9 (red) immunostaining. Nuclear Sox9+ staining in Amylase+ cells is characteristic of ADM in mutants (H'). (I) RTq-PCR of acinar markers. (J) H&E staining shows lymphocyte infiltration and lipomatosis in mutants. (K) RT-qPCR of immune infiltrates (*F4/80, CD2, CD19)*, cytokines (IL10) and chemokines (CCL2, CCL5, CXCXL10). (L, M) Macrophage

marker F4/80 (brown) immunostaining. (N, O) Adipocyte marker Fabp4 (green) immunostaining and (P) qRT-PCR of *PPARγ*. (Q, R) Masson's Trichrome staining. (S) RT-qPCR of *Col1A1*. (T, U) Vimentin (brown) immunostaining. (V) RT-qPCR of *SMA*, *Vimentin* (Vim), *N-Cad* and *E-Cad*. Scale bars: (B, C) 2 mm; (D-H, J, L-M, Q-U) 50 µm; (N, O) 100 µm. Nuclei are stained with DAPI (blue). Control, n≥3; Mutant, n≥3 for immunostainings and Control, n=8; Mutant, n=5 for RT-qPCR. ***P*<0.01; ****P*<0.001.

Figure 6. Ductal deletion of *Hnf1b* leads to enhanced signaling pathways that favor tumorigenesis. (A) RT-qPCR of YAP transcriptional targets. (B-E) CTGF (brown) immunohistochemistry. A strong ectopic CTGF staining is observed in acinar cells in mutants (C') in the epithelium of metaplastic ducts (D') and in PanIN (E'). (F) RT-qPCR of Notch pathway. (G, H) HEY2 immunohistochemistry. (I) RT-qPCR of *TGF-β1.* (J, K) Phospho-SMAD2 (Ser465, Ser467) immunohistochemistry. (L) RT-qPCR of *EGFR*. (M, N) Phospho-AKT (Ser473) immunohistochemistry. Nuclei were counterstained with Hematoxylin. Scale bars: 100 µm. Control, n≥3; Mutant, n≥3 for immunohistochemistry and Control, n=6; Mutant, n=5 for RT-qPCR. **P*<0.05; ***P*<0.01; ****P*<0.001.

Figure 7. Ductal deletion of *Hnf1b* leads to pancreatic intraepithelial neoplasia (PanIN) by 2 months. (A) H&E staining of mutant pancreata showing epithelial structures composed of columnar cells with abundant supranuclear cytoplasm and basally located nuclei. (B) Alcian blue staining. Columnar mutant epithelial cells revealed blue stained supranuclear mucin. (C) PanIN marker Claudin18 (brown) immunohistochemistry. (D) Sox9 (red) and GFP (green) immunostaining. Sox9+ ADM structures did not derived from Hnf1b-targeted GFP+ cells. (E) Quantification of the relative surface of acini, adipocytes, fibrosis/infiltrates, ADM and PanINs in mutants

(n=6). Scale bars: 100 µm. (Control, n≥3; Mutant, n≥3 for histology and immunohistochemistry).

Figure 8. **Ductal deletion of *Hnf1b* promotes PanIN progression in a Kras activated context.** Sox9-Cre^{ER};Hnf1b$^{fl/fl}$ Mutants were crossed with Elas-tTA; TetO-Flpase; Kras^{G12V} mice (referred to as Kras) to obtain Sox9-Cre^{ER};Hnf1b$^{fl/fl}$;Elas-tTA; TetO-Flpase; Kras^{G12V} (referred to as Mutant;Kras) that combined perinatal inactivation of Hnf1b in ducts and oncogenic activation of Kras^{G12V} in acinar cells. Analyses of the pancreata were performed at 5 months. (A) H&E staining. (B) Alcian Blue staining. (C) Claudin18 (brown) immunostaining. (D) Quantification of the surface of the lesions stained with Alcian Blue. (E) Quantification of the number of lesions per cm^2. (F) Quantification of the size of the lesions. (G-K) High grade PanINs in Mutant;Kras by H&E staining (G-J) and Alcian Blue staining (K). Some lesions present marked cytological and architectural atypia with the formation of branching papillae. Nuclei are enlarged and hyperchromatic with focal nuclear stratification. Scale bars: 100µm. Mutants n=5, Kras n=4, Mutant;Kras n= 3. **P*<0.05; ****P*<0.001.

Figure 9. **Adult Hnf1b inactivation in ductal cells does not lead to obvious perturbation of acinar homeostasis.** Tamoxifen was injected to 6-weeks old adult mice and analyses were performed at 2 months (A, B) or 5 months (C-F). (A) Mouse weight, pancreas weight and relative pancreas weight/body weight of 2-months old mice. (B) RT-qPCR of acinar markers at 2 months. (C) Mouse weight, pancreas weight and relative pancreas weight/body weight of 5-months old mice. (D) RT-qPCR of acinar markers at 5 months. (E, F) H&E staining of the pancreata at 5 months. Scale bars: 100µm. Control, n≥5; Mutants, n≥5. **P*<0.05.

Figure 10. Adult Hnf1b inactivation in ductal cells leads to impaired acinar regeneration and to neoplasia following cerulein-induced pancreatitis. (A) Analysis of *Hnf1b* inactivation efficiency by RT-qPCR. (B) RT-qPCR of *Amylase* at D0, D3 and D7. (C) RT-qPCR of acinar markers at D7. (D) RT-qPCR of inflammatory markers at D7. (E) H&E and Masson's Trichrome stainings (F, G) Amylase (green) and Sox9 (red) immunostaining showing widespread ADM at D7 in mutants. (H-I) H&E staining, (J, K) Alcian blue staining, (L, M) Claudin18 (brown) immunostaining, showing PanIN in mutants. Scale bars: (E) 50 µm; (F-M) 100 µm. Control, n≥5; Mutants, n≥5 for RT-qPCR and Control, n≥3; Mutants, n≥3 for histology and immunostainings. ***P*<0.01; ****P*<0.001.

ACCEPTED MANUSCRIPT

ACCEPTED MANUSCRIPT

Antibodies

Antigen	Host	Dilution	Reference
Amylase	Goat	1/50	Santa Cruz; sc-12821
Acetylated α-Tubulin	Mouse	1/300	Sigma; T6793
AKT-Phospho-S473	Mouse	1/100	Proteintech; 66444-1-Ig
Arl13b	Mouse	1/100	Antibodies Incorporated; 75-287
β-Catenin	Mouse	1/100	BD Biosciences; 610153
Claudin-18	Rabbit	1/250	ThermoFisher Scientific; 700178
CTGF	Rabbit	1/3000	Antibody Verify; AAS91519C
F4/80	Rat	1/500	BioLegend; 123102
Fabp4	Rabbit	1/200	Abcam; ab13979
GFP	Chicken	1/400	Aves Labs; GFP-1020
Hey2	Rabbit	1/100	Proteintech; 10597-1-AP
Hnf1b	Rabbit	1/50	Santa Cruz; sc-22840
Hnf6	Guinea pig	1/500	From Frederic Lemaigre's lab
Muc1	Hamster	1/100	ThermoFisher Scientific; HM-1630-PO
α-Smooth Muscle Actin	Mouse	1/50	Sigma; C6198
Pan-CK	Mouse	1/100	Sigma; C1801
Phospho-Histone H3	Mouse	1/300	Cell Signaling; 9706
Phospho-SMAD2 (Ser435, Ser 467)	Rabbit	1/150	ThermoFisher Scientific; 44-244G
PKCzeta	Rabbit	1/500	Santa Cruz; sc-216
Sox9	Rabbit	1/100	Millipore; AB5535
SPP1/ Osteopontin	Goat	1/100	R&D Systems; AF808
Vimentin	Goat	1/100	Santa Cruz; sc-7557
YAP	Mouse	1/50	Santa Cruz; sc-101199

ACCEPTED

ACCEPTED MANUSCRIPT

Name	Forward Sequence (5'-3')	Reverse Sequence (5'-3')
Amylase	CTGGGTTGATATTGCCAAGG	TGCACCTTGTCACCATGTCT
Birc5	CTGATTTGGCCCAGTGTTTT	CAGGGGAGTGCTTTCTATGC
Ccl2	AGCTGTAGTTTTTGTCACCAAGC	GTGCTGAAGACCTTAGGGCA
Ccl5	CCTCACCATATGGCTCGGAC	ACGACTGCAAGATTGGAGCA
CD2	AGGATTCTGGAGAGGGTCTCA	TCGCCTCACACTTGAATGGT
CD19	GTCATTGCAAGGTCAGCAGTG	GGGTCAGTCATTCGCTTCCT
Ck19	ACCCTCCCGAGATTACAACC	TCTGAAGTCATCTGCAGCCA
Col1A1	ACCTCAAGATGTGCCACTC	TGCTCTCTCCAAACCAGAC
CPA	CAACCCCTGCTCAGAAACTTACC	TGGACTTGACCTCCACTTCAGA
CTGF	GCCAACCGCAAGATCGGAGTGT	ACGGCCCCATCCAGGCAA
CXCL10	GCTGCCGTCATTTTCTGC	TCTCACTGGCCCGTCATC
Cyclophilin A	CAGGTCCTGGCATCTTGTCC	TTGCTGGTCTTGCCATTCCT
Cyr61	TCTGTGAAGTGCGTCCTTGT	CTGGTTCTGGGGATTTCTTG
Cys1	AGAGGAGCTCATGGCGAGCATT	GCCTGTGGCACAGATGCCAAGA
E-Cad	GCAGTCCCGGCTTCAGTTCC	GCCGGCCAGTGCATCCTT
EGFR	GCAGGGAGTGCGTGGAGAAATG	GTTGTCTGGTCCCCTGCCTGTA
F4/80	CTTTGGCTATGGGCTTCCAGTC	GCAAGGAGGACAGAGTTTATCGTG
Hes1	CAAAGACGGCCTCTGAGCAC	CCTTCGCCTCTTCTCCATGAT
Hey2	AGCGCCCTTGTGAGGAAACGA	TGTAGCGTGCCCAGGGTAATTG
Hnf1a	GTGTAACTGCACAGGAGGCAAA	TTCTCACGTGTCCCAAGACCTA
Hnf1b	GGCCTACGACCGGCAAAAGA	GGGAGACCCCTCGTTGCAAA
Hnf6	CAAATCACCATCTCCCAGCAG	CAGACTCCTCCTCCTGGCATT
IL10	CAGAGCCACATGCTCCTAGA	TGTCCAGCTGGTCCTTTGTT
Jag1	TGCCCTCCAGGACATAGTGG	ACTCTCCCCATGGTGATGCA
LAMC2	ATTGGCTCCCAACCCAGCAGA	ACAGCTGCCATCACCTCGACA
Mist1	TGGGCCTCCAGATCTCACCAA	CGTCACATGTCAGGTTTCTCTGCT
Muc1	CTCTGGAAGACCCCAGCTCCAA	CCACGGAGCCTGACCTGAACT
N-Cad	GCTGACCACGCTCACTGCT	ATCTGCCCATTCACGGGGTCTA
Notch2	CCTGCCAGGTTTTGAAGGGA	GGGCAGTCGTCGATATTCCG
Nr5a2	CTGCTGGACTACACGGTTTGC	CTGCCTGCTTGCTGATTGC
P8/Nupr1	GAGAAGCTGCTGCCAATACC	GTGTGGTGTCTGTGGTCTGG
Pkd1	GCTGCATGCCAGTTCTTTTG	TTTTAAAGTGCAGAAGCCCCA
Pkhd1	TGCTCCTCAGGCAGGCAATCG	ACCTGTACCCTGGGGTGGCTT
PPARg	GATGGAAGACCACTCGCATT	AACCATTGGGTCAGCTCTTG
Prox1	CGCAGAAGGACTCTCTTTGTC	GATTGGGTGATAGCCCTTCAT
Ptf1a	TTCCTGAAGCACCTTTGACAGA	ACGGAGTTTCCTGGACAGAGT
Rbpj	GTTTTGGCGAGAGTTTGTGGAAGAT	TGGAGGCCGCTCACCAAACT
SMA	GACGCTGCTCCAGCTATGT	AGTTGGTGATGATGCCGTGT
Sox9	AAGCCGACTCCCCACATTCCTC	CGCCCCTCTCGCTTCAGATCAA
Spp1	CCCTCCCGGTGAAAGTGACTGA	GCACCAGCCATGTGGCTATAGG
TGF-b1	AGAGGTCACCCGCGTGCTAAT	GGGCACTGCTTCCCGAATGTC
Vimentin	GGGAGAAATTGCAGGAGGAG	ATTCCACTTTGCGTTCAAGG

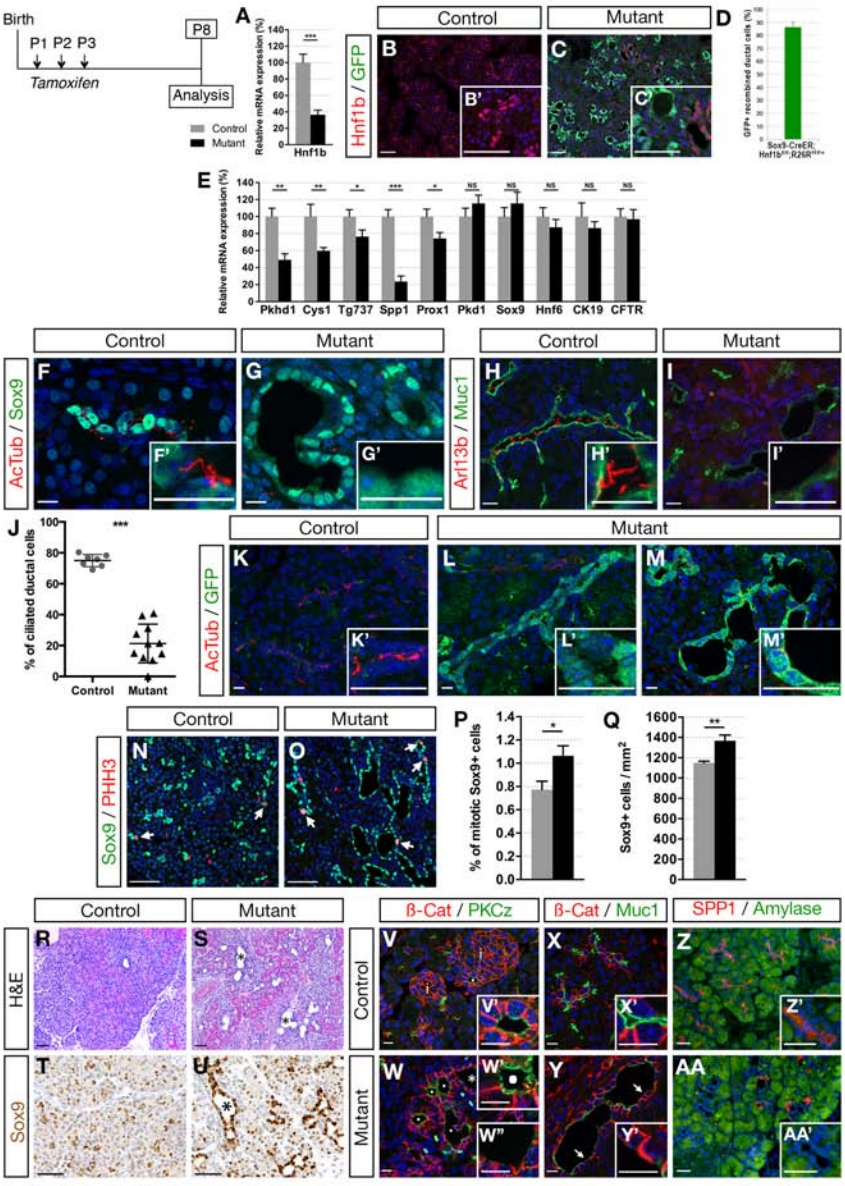
Birth
P1 P2 P3
P8
Tamoxifen
Analysis
Control
Mutant
A
Relative mRNA expression (%)
Hnf1b
Hnf1b / GFP
Control
Mutant
B
B'
C
C'
D
GFP+ recombined ductal cells (%)
Sox9-CreER; Hnf1b^fl/fl; R26R^YFP/+
E
Relative mRNA expression (%)
Pkhd1
Cys1
Tg737
Spp1
Prox1
Pkd1
Sox9
Hnf6
CK19
CFTR
AcTub / Sox9
F
F'
G
G'
Arl13b / Muc1
H
H'
I
I'
J
% of ciliated ductal cells
AcTub / GFP
K
K'
L
L'
M
M'
Sox9 / PHH3
N
O
P
% of mitotic Sox9+ cells
Q
Sox9+ cells / mm²
H&E
R
S
Sox9
T
U
ß-Cat / PKCz
ß-Cat / Muc1
SPP1 / Amylase
V
V'
X
X'
Z
Z'
W
W'
W''
Y
Y'
AA
AA'

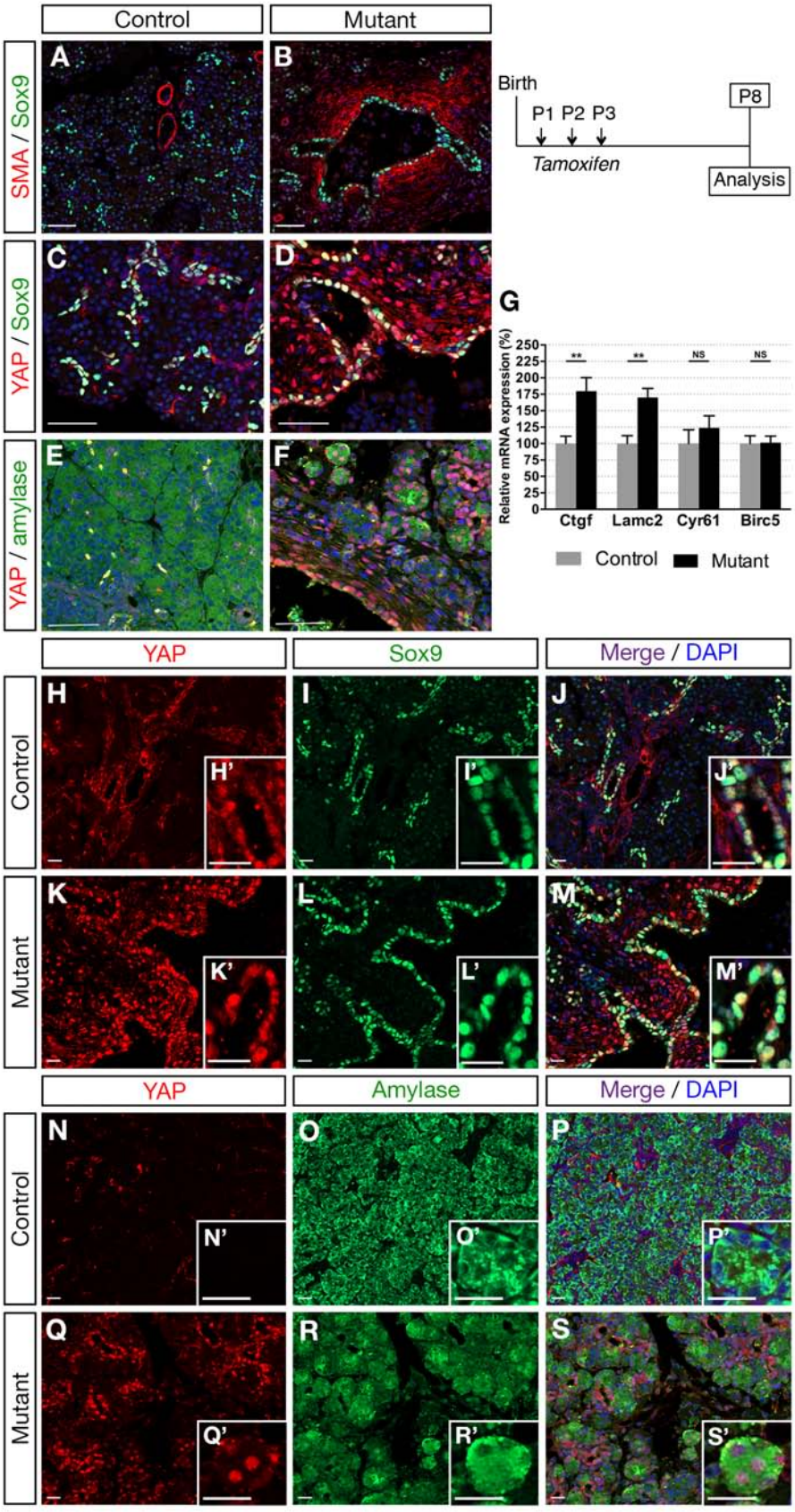
Control
Mutant
SMA / Sox9
YAP / Sox9
YAP / amylase
A
B
C
D
E
F
Birth
P1 P2 P3
Tamoxifen
P8
Analysis
G
Relative mRNA expression (%)
250
225
200
175
150
125
100
75
50
25
0
**
**
NS
NS
Ctgf
Lamc2
Cyr61
Birc5
Control
Mutant
YAP
Sox9
Merge / DAPI
Control
Mutant
H
I
J
K
L
M
H'
I'
J'
K'
L'
M'
YAP
Amylase
Merge / DAPI
Control
Mutant
N
O
P
Q
R
S
N'
O'
P'
Q'
R'
S'

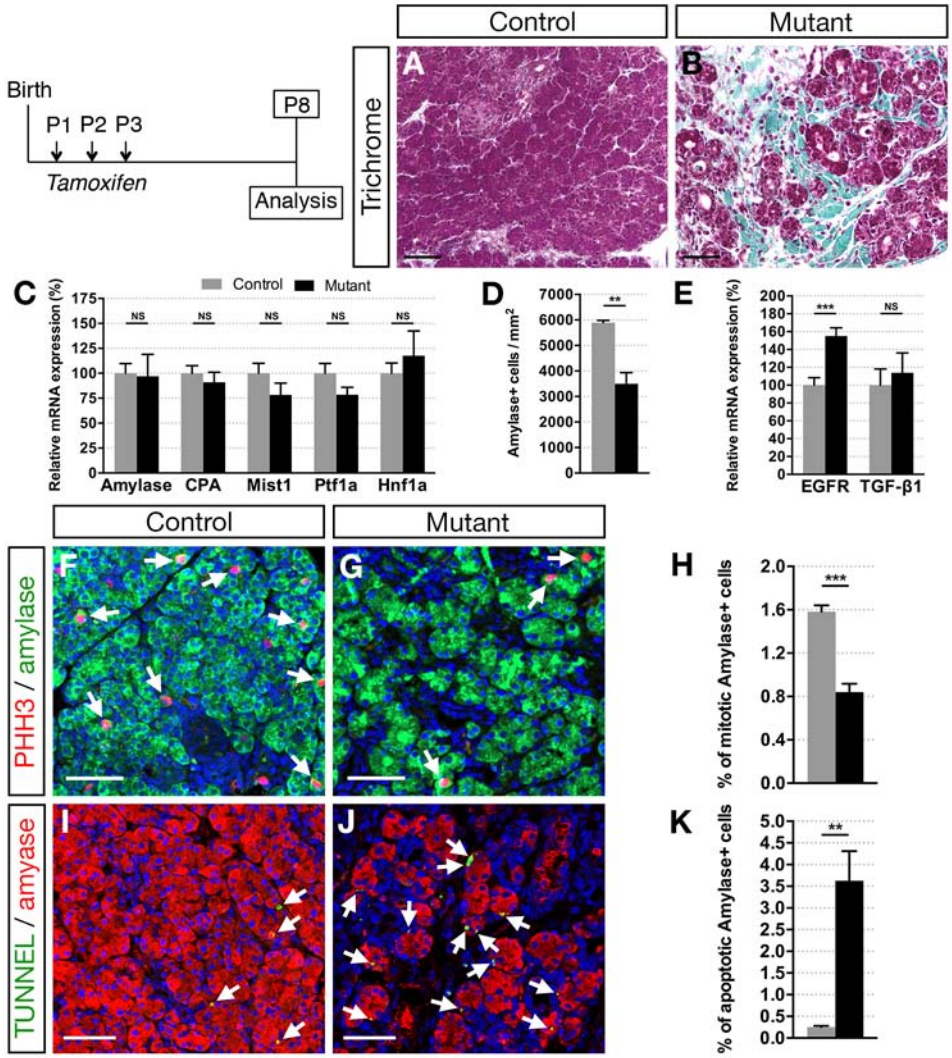

ACCEPTED MANUSCRIPT

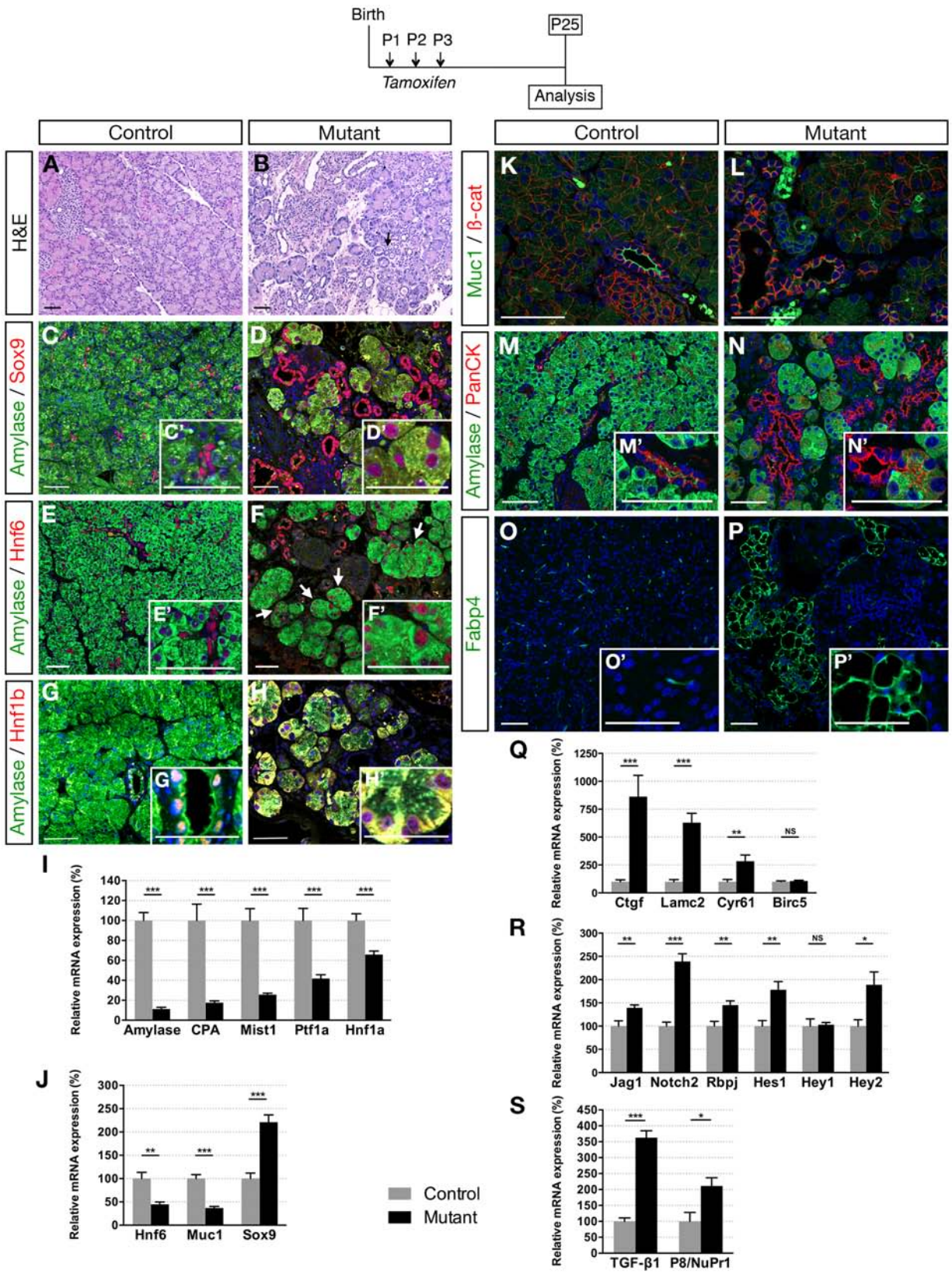

ACCEPTED MANUSCRIPT

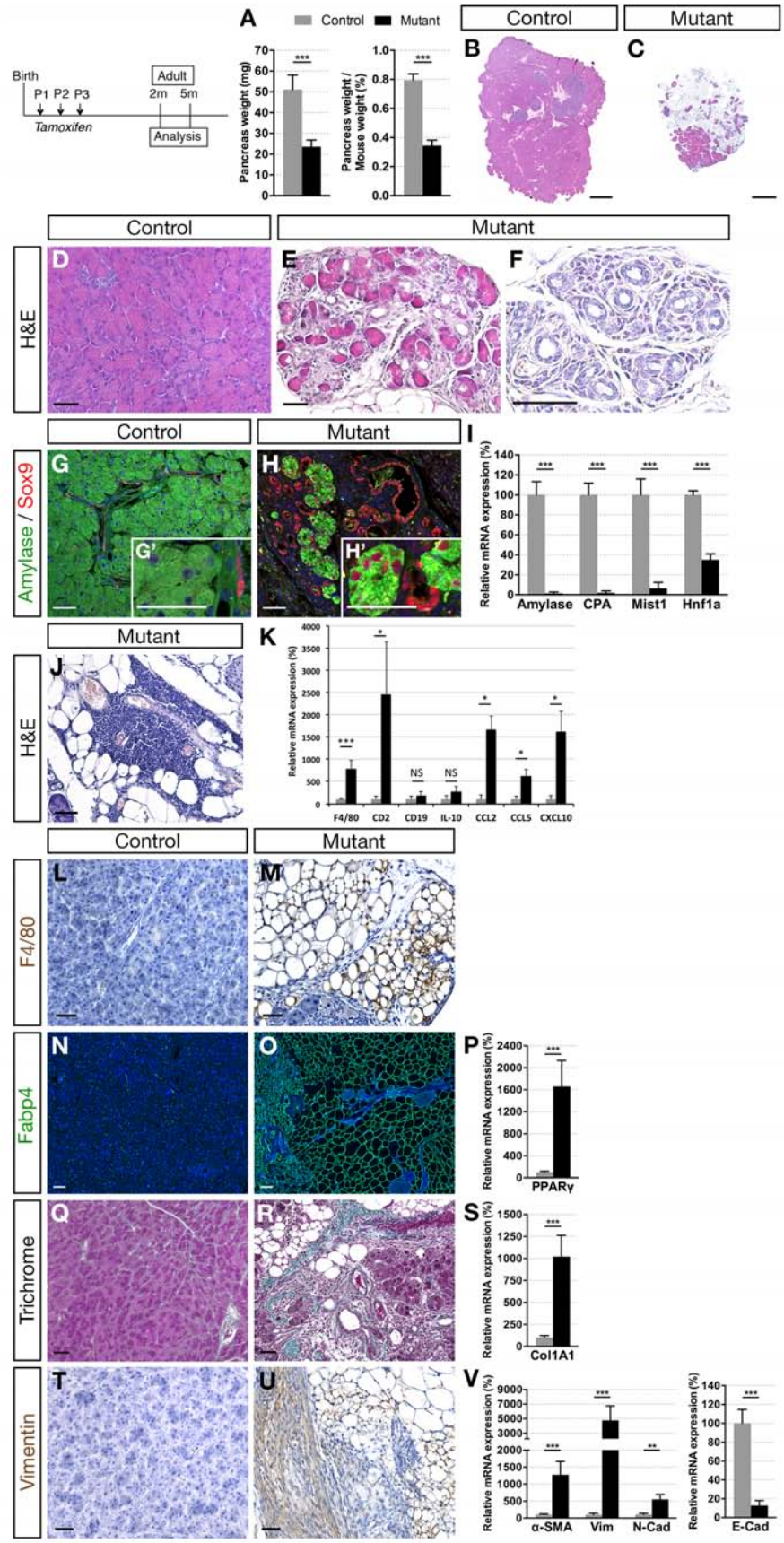
A
Control
Mutant
Birth
P1 P2 P3
Tamoxifen
Adult
2m 5m
Analysis
Pancreas weight (mg)
Pancreas weight / Mouse weight (%)
B
C
Control
Mutant
H&E
D
E
F
Amylase / Sox9
G
G'
H
H'
I
Relative mRNA expression (%)
Amylase
CPA
Mist1
Hnf1a
J
K
F4/80
CD2
CD19
IL-10
CCL2
CCL5
CXCL10
NS
L
M
F4/80
N
O
Fabp4
P
PPARγ
Q
R
Trichrome
S
Col1A1
T
U
Vimentin
V
α-SMA
Vim
N-Cad
E-Cad

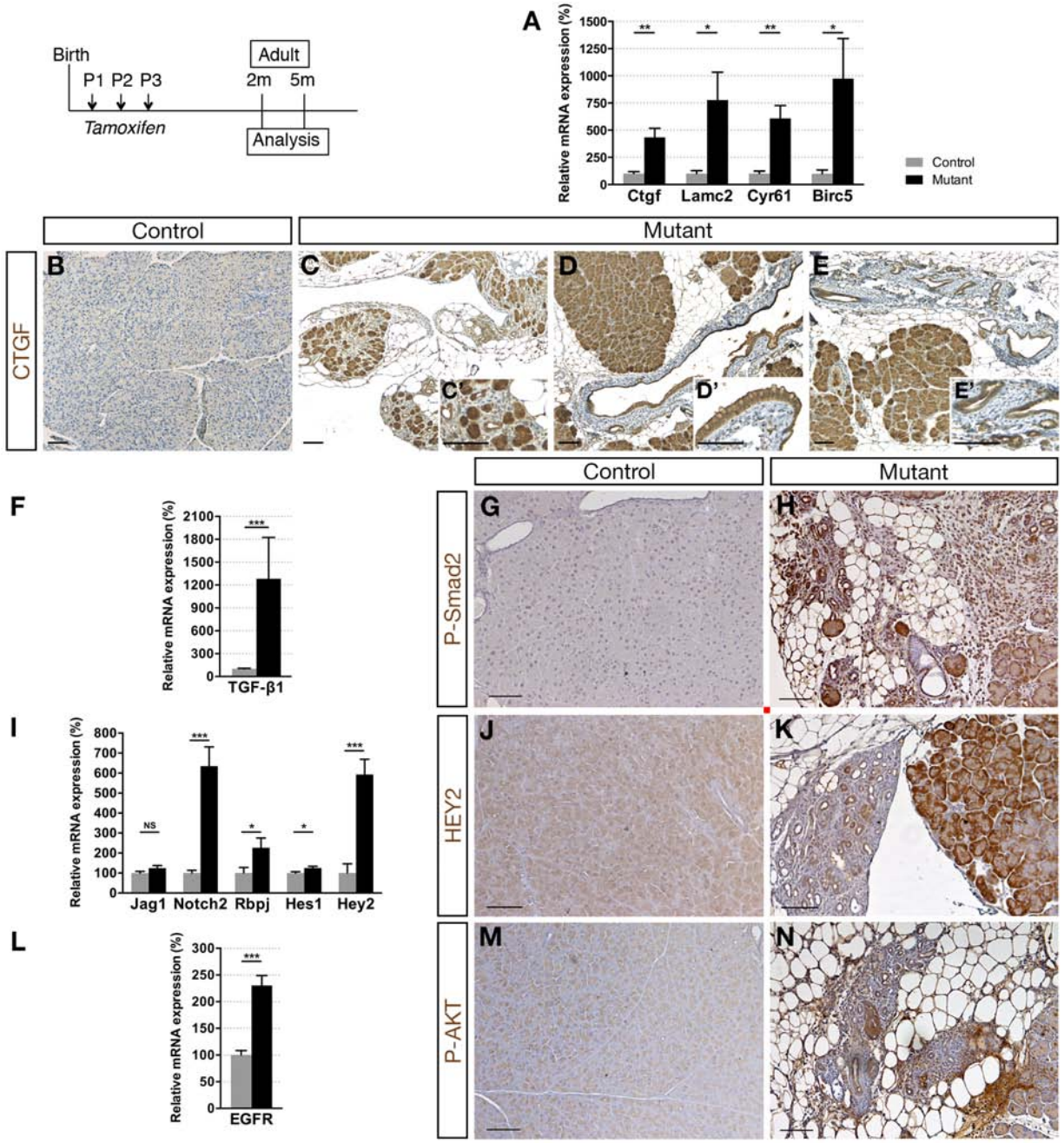
Birth
P1 P2 P3
Tamoxifen
Adult
2m 5m
Analysis
A
Relative mRNA expression (%)
Ctgf
Lamc2
Cyr61
Birc5
Control
Mutant
Control
Mutant
CTGF
B
C
C'
D
D'
E
E'
F
Relative mRNA expression (%)
TGF-β1
I
Relative mRNA expression (%)
Jag1
Notch2
Rbpj
Hes1
Hey2
NS
L
Relative mRNA expression (%)
EGFR
Control
Mutant
P-Smad2
G
H
HEY2
J
K
P-AKT
M
N

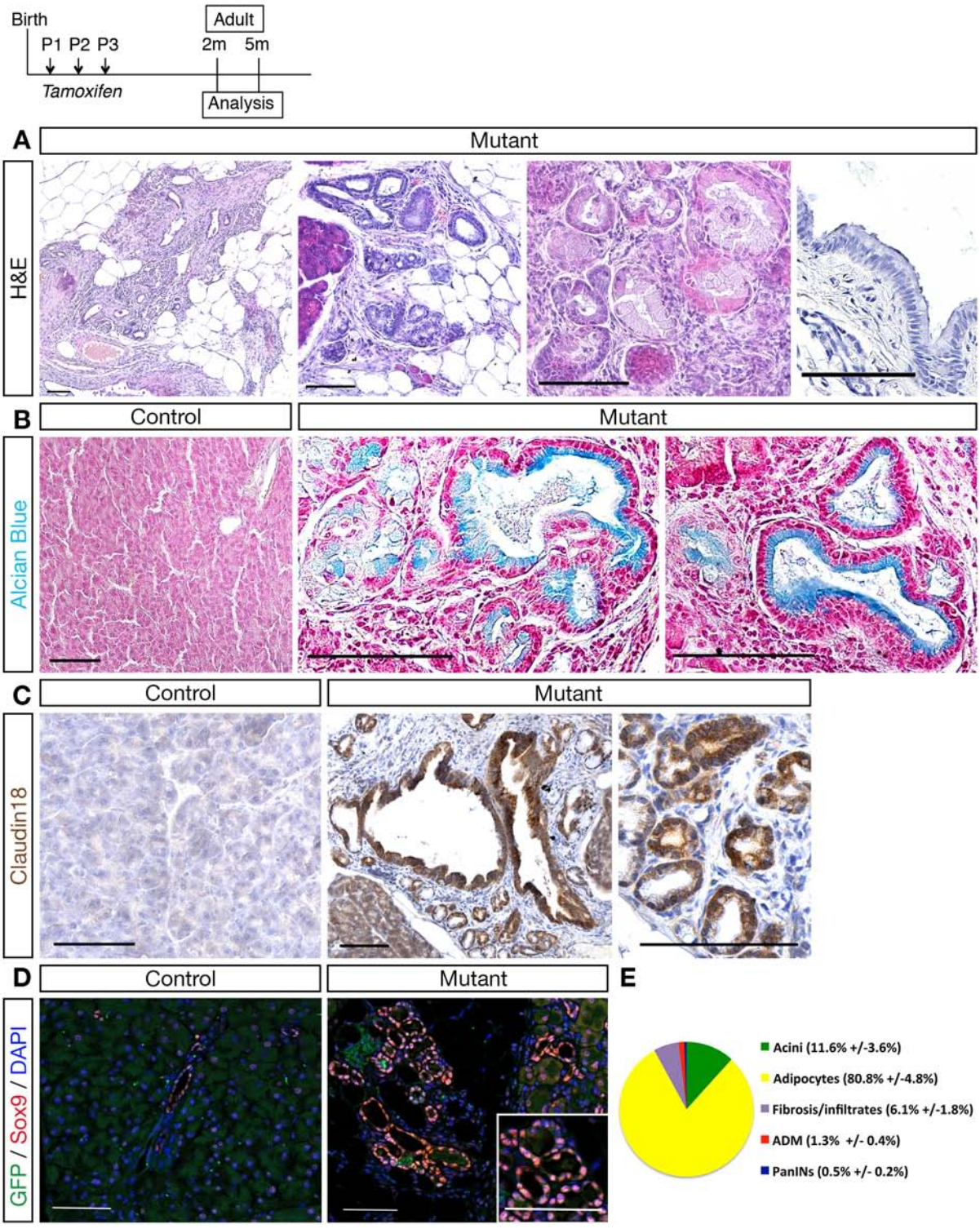
Birth
P1 P2 P3
Tamoxifen
Adult
2m 5m
Analysis
A
Mutant
H&E
B
Control
Mutant
Alcian Blue
C
Control
Mutant
Claudin18
D
Control
Mutant
GFP / Sox9 / DAPI
E
Acini (11.6% +/-3.6%)
Adipocytes (80.8% +/-4.8%)
Fibrosis/infiltrates (6.1% +/-1.8%)
ADM (1.3% +/- 0.4%)
PanINs (0.5% +/- 0.2%)

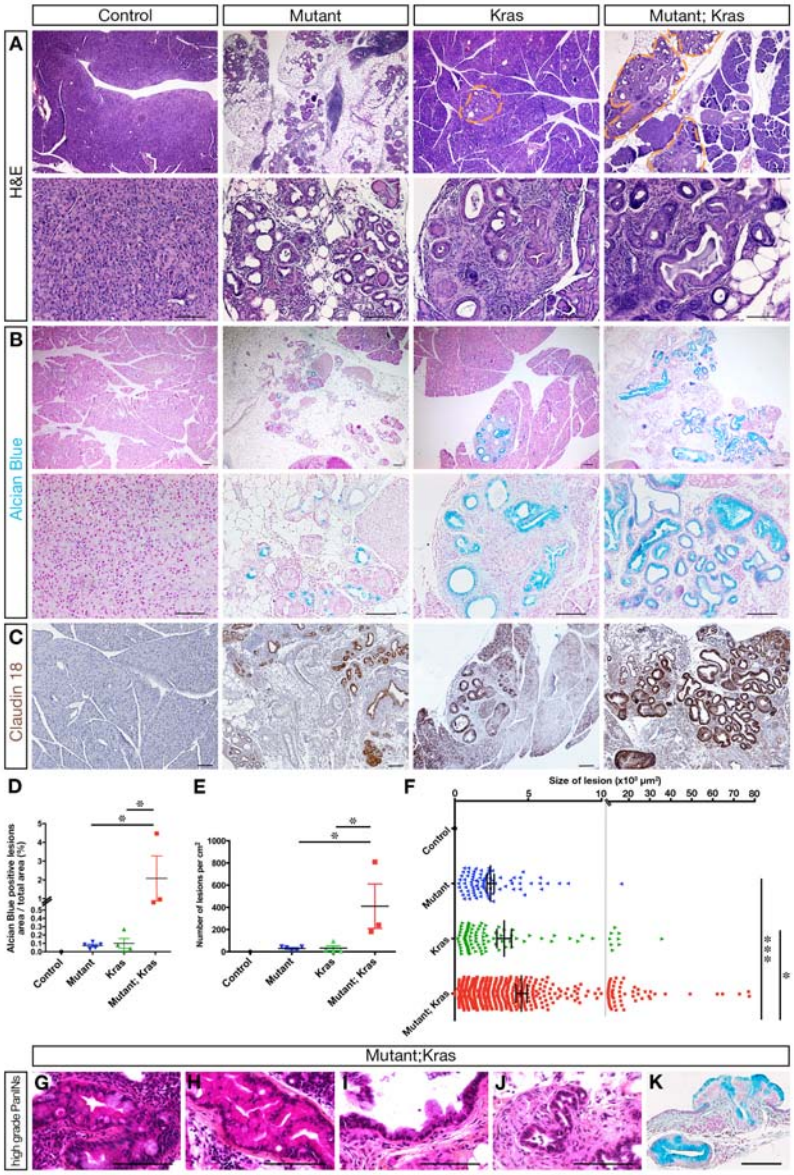

ACCEPTED MANUSCRIPT

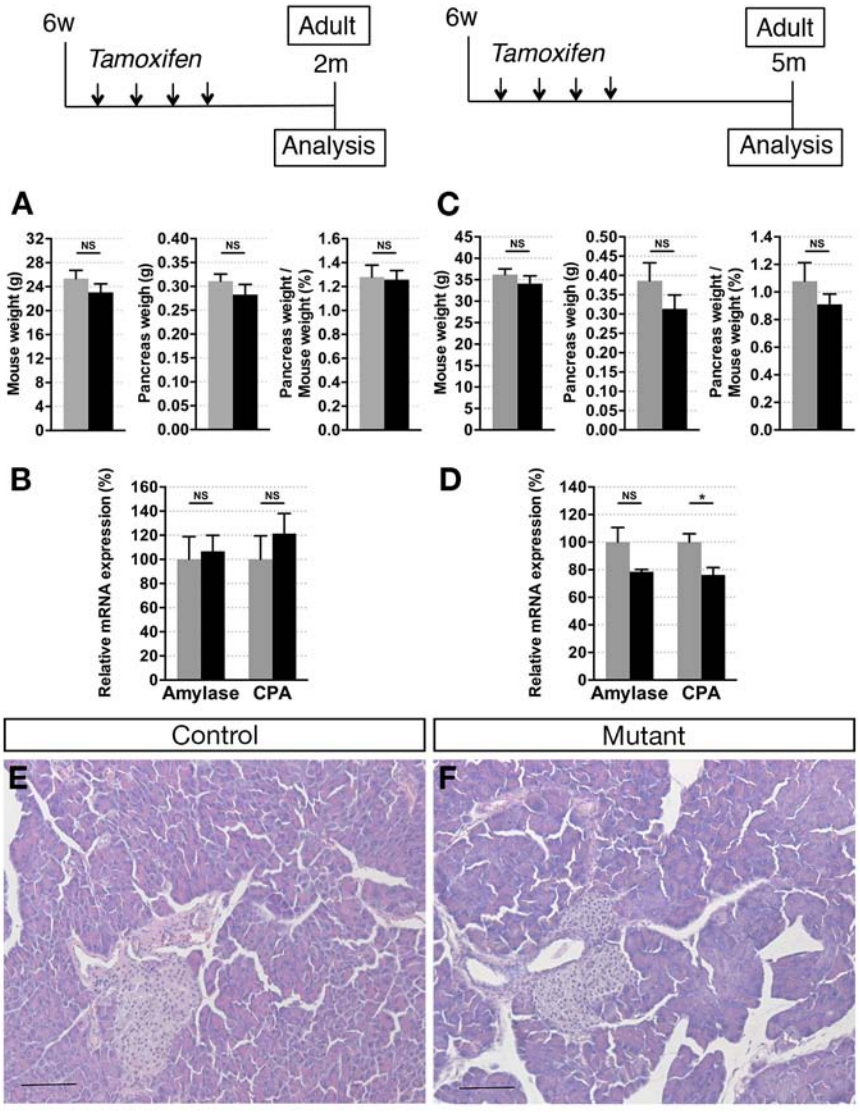

ACCEPTED MANUSCRIPT

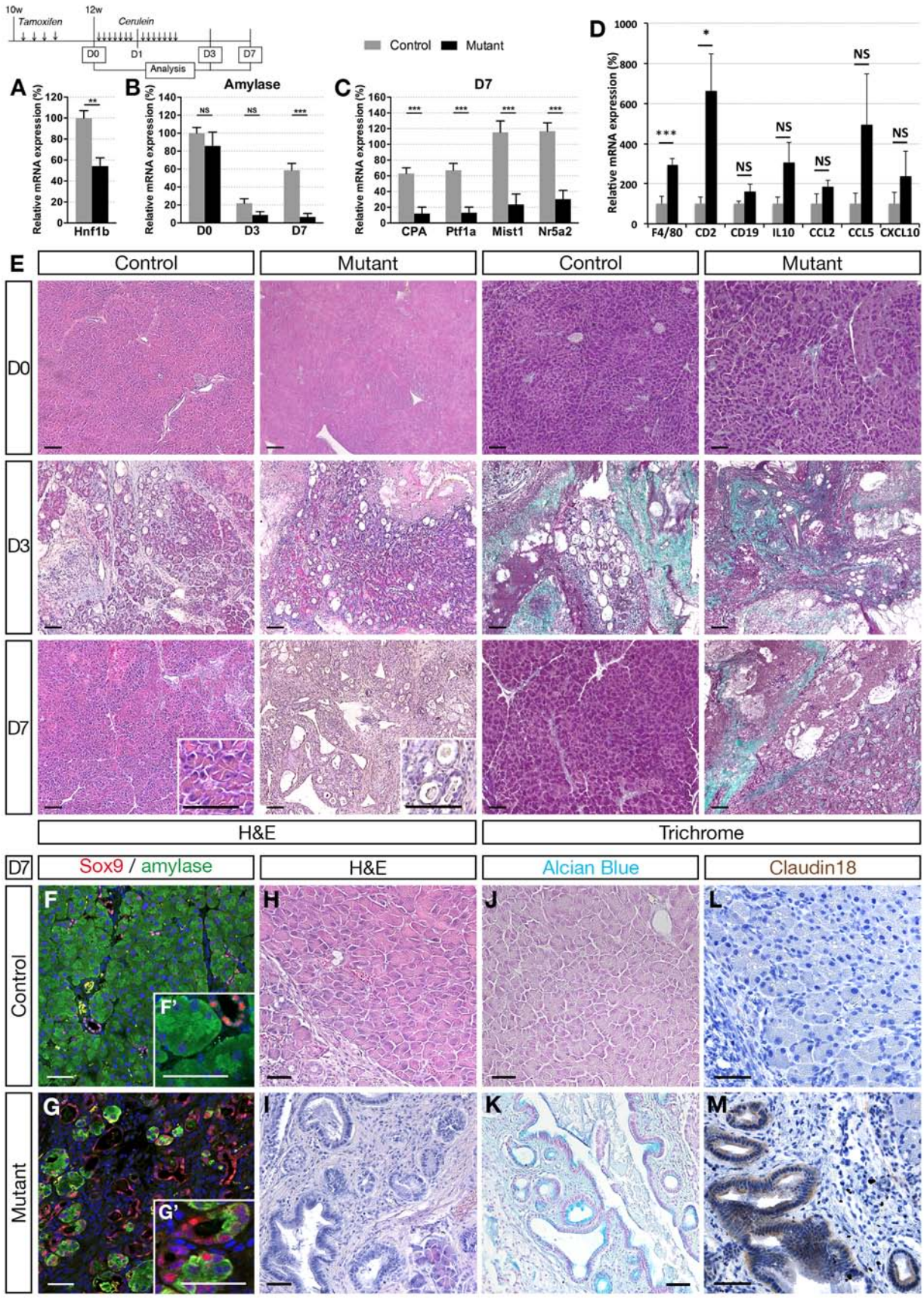
10w
Tamoxifen
12w
Cerulein
D0
D1
D3
D7
Analysis
A
Relative mRNA expression (%)
Hnf1b
B
Amylase
D0
D3
D7
C
D7
Control
Mutant
CPA
Ptf1a
Mist1
Nr5a2
D
F4/80
CD2
CD19
IL10
CCL2
CCL5
CXCL10
NS
E
Control
Mutant
D0
D3
D7
H&E
Trichrome
Sox9 / amylase
H&E
Alcian Blue
Claudin18
F
F'
G
G'
H
I
J
K
L
M

ACCEPTED MANUSCRIPT

ACCEPTED MANUSCRIPT